C. CEYLAN

DESIGN AND OPTIMIZATION OF SOLAR BASED HYBRID POWER SYSTEM

THE GRADUATE SCHOOL OF NATURAL AND APPLIED SCIENCES
OF
ATILIM UNIVERSITY

CEREN CEYLAN

A MASTER OF SCIENCE
THESIS
IN
THE DEPARTMENT OF ELECTRICAL AND ELECTRONICS ENGINEERING

JULY 2020

ATILIM UNIVERSITY 2020

DESIGN AND OPTIMIZATION OF SOLAR BASED HYBRID POWER SYSTEM

A THESIS SUBMITTED TO
THE GRADUATE SCHOOL OF ELECTRICAL AND ELECTRONICS ENGINEERING
OF
ATILIM UNIVERSITY
BY
CEREN CEYLAN

IN PARTIAL FULFILLMENT OF THE REQUIREMENTS FOR
THE DEGREE OF MASTER OF SCIENCE IN
ELECTRICAL AND ELECTRONICS ENGINEERING

JULY 2020

Approval of the Graduate School of Natural and Applied Sciences, Atilim University.

Prof. Dr. Ali KARA
Director

I certify that this thesis satisfies all the requirements as a thesis for the degree of **Master of Science in Electrical and Electronics Engineering Department, Atilim University**.

Assoc. Prof. Dr. Kemal Efe ESELLER
Head of Department

This is to certify that we have read the thesis DESIGN AND OPTIMIZATION OF SOLAR BASED HYBRID POWER SYSTEM submitted by CEREN CEYLAN and that in our opinion it is fully adequate, in scope and quality, as a thesis for the degree of Master of Science.

Assoc. Prof. Dr. Yılser DEVRİM
Supervisor

Examining Committee Members:

Prof. Dr. Ayhan ALBOSTAN
Energy Systems Engineering, Atilim University

Assoc. Prof. Dr. Yılser DEVRİM
Energy Systems Engineering, Atilim University

Prof. Dr. Adem ACIR
Energy Systems Engineering, Gazi University

Date: JULY 17, 2020

I declare and guarantee that all data, knowledge and information in this document has been obtained, processed and presented in accordance with academic rules and ethical conduct. Based on these rules and conduct, I have fully cited and referenced all material and results that are not original to this work.

Name, Last Name: CEREN CEYLAN
Signature:

ABSTRACT

DESIGN AND OPTIMIZATION OF SOLAR BASED HYBRID POWER SYSTEM

Ceylan, Ceren
M.S., Department of Electrical and Electronics Engineering
Supervisor: Assoc. Prof. Dr. Yılser DEVRİM

JULY 2020, 62 pages

With the developing technology and increasing World population, energy demand is increasing. Since fossil fuels are running out day by day, renewable energy sources have been used to produce clean energy. The most preferred renewable energy source is the Sun that cannot be used on cloudy days and nights. Also, the most important disadvantages of solar energy are storage. In these conditions, fuel cells are used to meet the energy needs and ensure continuity. Due to their short start-up times and high efficiency, fuel cells have become popular. Hydrogen (H_2), the most common element in the universe, is used as a fuel in fuel cells. H_2 is not an energy source, but it is a very good energy carrier. When H_2 used as a fuel, water or water vapor is released. During the production of energy, there is no harmful gases and chemicals which pollute the environment and increase the greenhouse effect which proves that it is environmentally friendly.

In this thesis, 2.4 kW Proton Exchange Membrane Fuel Cell (PEMFC), which was operated for 5 hours a day, was designed to meet the energy needs of a greenhouse in Şanliurfa. The electrolyzer was designed to produce H_2 for PEMFC and the electricity demand for the operation of the electrolyzer was supplied from 80 photovoltaic (PV) cells. The produced H_2 was stored in storage tanks for use in PEMFC. At the end of 365 days, total of 430 kg H_2 was stored with designed system. Also, heat was released when PEMFC operates and it was approximately 20 kW per day. This heat must be removed to ensure that the PEMFC's safety and high efficiency. The generated heat

produced from PEMFC was removed with the help of the heat exchanger. In this process, while the temperature of the PEMFC cooling water, which was heated by the heat removal, decreases to 34 ^{o}C, the temperature of the water to be used for the heating of the greenhouse is increased up to 61 ^{o}C.

The ratio of investment, operation, and maintenance costs to the amount of energy produced by hybrid energy system during operation gives the levelized cost of energy. It was calculated 1.77 $/kWh for this hybrid energy system.

Keywords: Hybrid Systems, Photovoltaics, PEMFC, MATLAB/Simulink

ÖZ

GÜNEŞ ESASLI HİBRİT GÜÇ SİSTEMLERİNİN TASARIMI VE OPTİMİZASYONU

Ceylan, Ceren
Yüksek Lisans, Elektrik Elektronik Mühendisliği
Tez Yöneticisi: Doç. Dr. Yılser DEVRİM

HAZİRAN 2020, 62 sayfa

Gelişen teknoloji ve artan Dünya nüfusuyla birlikte enerji talebi de artmaktadır. Fosil yakıtların günden güne tükenmesi nedeniyle, temiz enerji üretmek için yenilenebilir enerji kaynaklarını kullanılmaya başlanmıştır. En çok tercih edilen yenilenebilir enerji kaynağı olan güneş enerjisi bulutlu günlerde ve gecelerde kullanılamaz. Ayrıca güneş enerjisinin en büyük dezavantajı depolanma sorunun olmasıdır. Bu şartlarda enerji ihtiyacını karşılamak ve sürekliliği sağlamak için yakıt pilleri kullanılır. Kısa başlangıç sürelerinin olması ve yüksek verimlilikleri nedeniyle yakıt pilleri popüler hale geldi. Evrende en çok bulunan element olan Hidrojen (H_2), yakıt pillerinde yakıt olarak kullanılır. H_2 enerji kaynağı değildir ancak çok iyi bir enerji taşıyıcısıdır. Yakıt olarak kullanıldığında su ya da su buharı ortaya çıkar. Enerji üretimi sırasında, çevreyi kirleten ve sera etkisini arttıran kimyasallar ve zararlı gazlar yoktur ve bu da çevre dostu olduğunu kanıtlar.

Bu tez çalışmasında, Şanlıurfa'da bulunan bir seranın enerji ihtiyacını karşılamak için günde 5 saat çalıştırılacak olan 2.4 kW Proton Değişim Membran Yakıt Pili (PEMFC) tasarlanmıştır. PEMFC'nin gereksinimi olan H_2'yi üretmek için elektrolizör dizayn edilmiş ve elektrolizörün çalışması için gerekli olan elektrik 80 adet fotovoltaik (PV) modülden sağlanmıştır. Sistemde üretilen H_2 PEMFC'de kullanılmak üzere tanklarda depolanır. Tasarlanan sistemde bir yılın sonunda toplam 430 kg H_2 depolanmıştır. Bunun yanı sıra PEMFC çalışırken ısı ortaya çıkar ve bir günlük çalışmada yaklaşık olarak 20 kW ısı üretilmektedir. Bu ısı PEMFC'nin güvenliği ve yüksek verimliliğin

sağlanması için uzaklaştırılmalıdır. Tasarlanan sistemde PEMFC tarafından üretilen ısı bir ısı değiştiricisi yardımıyla uzaklaştırılmaktadır. Bu işlemde ısı uzaklaştırılması ile ısınan PEMFC soğutma suyunun sıcaklığı 34 ^{o}C'ye kadar düşerken, seranın ısınması için kullanılacak suyun ısısını 61 ^{o}C'ye kadar çıkarılmıştır.

Yatırım, işletme ve bakım maliyetinin, hibrit enerji sisteminin çalışma süresince ürettiği enerji miktarına oranı seviyelendirilmiş enerji maliyetini verir. Bu sisteminin seviyelendirilmiş enerji maliyeti 1.77 $/kWh olarak hesaplanmıştır.

Anahtar Kelimeler: Hibrit Sistemler, Fotovoltaik, PEM Yakıt Pili, MATLAB/Simulink

To my family

ACKNOWLEDGMENTS

I would like to express gratitude to supervisor Assoc. Prof. Dr. Yılser Devrim who is guiding in the determination of this topic, during the thesis writing process, analysis, interpretation, and evaluation of the data and who does not withhold her teaching about completing my work.

I thank to Prof. Dr. Ayhan Albostan for his valuable comments and suggestions. He guided me at a deadlock moment and allowed me to look through a new window.

I would like to thank to my cousin Şevval Kılıçoğlu who helps and always supports me. I should also thank to Yağmur Budak for answering my questions.

Special thanks to the Mone Tarım for supporting this study.

I am grateful to Yalçın Zaim who is the builder of my academic career and supported me all over for years.

My sincere thanks to Yiğit Tüfekçi who always supports me, shows understanding and helps me to complete my thesis.

Last but not least, I would like to extend my thanks to my family who have never spared their financial and moral support from me throughout my education.

TABLE OF CONTENTS

LIST OF TABLES

TABLE

LIST OF FIGURES

FIGURE

LIST OF SYMBOLS

I_L	:	Photogenerated current
I_D	:	Diode current
I_{SH}	:	Shunt current
I_0	:	Reverse saturation current
T_{cell}	:	Absolute temperature of cell in Kelvin.
η_{Cath}	:	Overpotential at the cathode
η_{An}	:	Overpotential at the anode
R_A	:	Specific ohmic resistance
V_{act}	:	The activation polarization losses
V_{ohm}	:	The ohmic (resistive) losses
V_{conc}	:	The concentration polarization losses
$P_{el,min}$	:	The minimum power of electrolyzer
$G_{I,ref}$	:	The reference solar irradiation of PV
G_I	:	Solar irradiance
$P_{PV,max}$	:	The maximum power of PV cell
μ_p	:	The power thermal coefficient
T_a	:	Ambient temperature
$T_{c,ref}$	:	PV cell temperature at standard conditions
V_{elec}	:	The voltage of electrolyzer
m_{el}	:	Molar flowrate of produced H_2 by electrolyzer
η_{dc}	:	Efficiency of DC generator

CHAPTER 1

1. INTRODUCTION

1.1. Energy Systems

Energy is one of the most important factors that affect and shape our daily life. The need for energy resources depends on the world population and the growth of industrial activities. Using of energy resources in efficiently and control over them have gained importance according to energy demand. Successful implementation of energy management has become a priority issue. The energy indicators of a country's living standards are per capita consumption of total energy along with the energy available in that area. In terms of living standards, it is desired that the energy density of that country is low and the total energy consumption per person is high.

Besides the benefits of energy for humanity, it has become phenomenon that especially harms natural life. Greenhouse effect which is also known global warming is only one of the damages. Intense expending of energy leads to global warming and it affects our future. Most of energy need is provided from fossil fuel (coal, natural gas, oil) in the last century. Fossil fuels are limited and have negative effects such as global warming on the environment. The cost of fuel and fuel transformation to the energy producing system are very expensive. For these reasons, countries have turned to the search for energy resources which are clean environmentally friendly and renewable [1]. Today, reducing the dependence on fossil fuels is aimed to meet energy needs. Scientific studies on renewable energy resources have been accelerated.

1.2. Renewable Energy Systems

Renewable energy is unlimited, can renew itself continuously and inexhaustible when it is used. Solar, wind, geothermal, tidal, biomass etc. are examples of renewable energy resources. Their technologies exist naturally in the world without human

contribution. They enable to us in order to convert their energy into usable energy. The energy carried by the sun rays, the energy of wind, the heat of earth and earth's core, plant's own energies and more known-unknown energy forms are converted into usable forms of energy. The most important advantages of all renewable energy sources are lowering carbon dioxide emission levels, thereby improving air quality and is to protect the environment [2].

Theoretically, the potential of renewable energy sources is technically higher than the world energy needs. However, evaluating this energy potential and converting it into energy supply is not always in lossless form for some technical and economic reasons. In other words, installation costs are very high and energy transmission may not be efficient [3].

CHAPTER 2

2. OVERVIEW OF HYBRID POWER SYSTEM

2.1. Hybrid Power Systems

None of the renewable energy sources can provide energy alone in all kinds of natural events and weather conditions. Eliminate this problem, more than one energy generation systems should be used and these systems are called as hybrid systems [4]. The purposes of these systems are that increasing the efficiency and providing that to meet the energy needs of the system in the absence or decrease of one of the resources. For example, the sun which is the most popular renewable energy resource is not available on cloudy days and at nights. In order to provide energy continuity, it is combined with other energy resources such as battery, fuel cell, electrolyzer, wind...

2.1.1. Photovoltaic-Battery Energy System

Energy coming from solar energy is not stable according to the intermittent nature of it. Electricity generation can be done with PV-battery hybrid energy system where sunshine is abundant. The methodology of PV-battery hybrid energy system is that, the electricity is generated by PV cells and it is stored in battery [5]. The basic schematic of PV-battery hybrid energy system is shown in 2.1. Battery usage increase the efficiency of system through storing excess PV generation and supplying consumption when it is need [6].

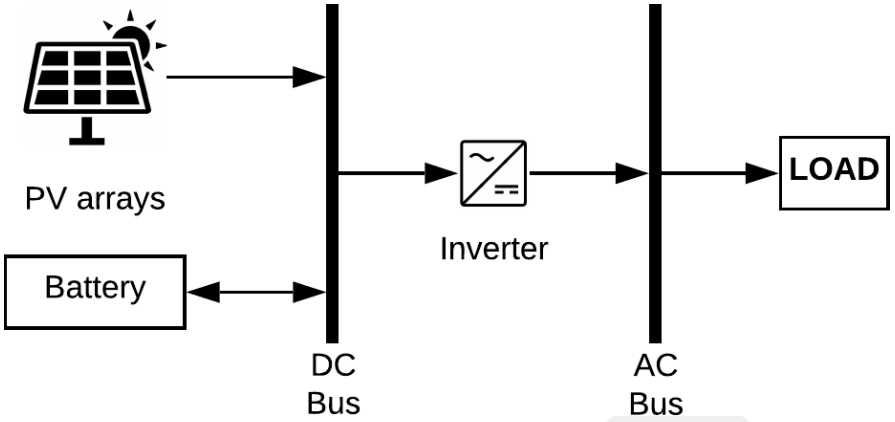

Figure 2.1: Schematic of a PV-battery hybrid energy system

2.1.2. Photovoltaic-Battery-Fuel Cell Hybrid Energy System

Usually, unused energy produced by PV cell is stored in a battery and it is used when sun is not available such as night or cloudy days. However, battery storing cost is very high for large amounts of energy and long term storage is not possible. Lifetime of batteries is limited. At this point, H_2 energy is combined with PV system and many studies have been done in this field. PV-FC hybrid system is considered one of the best alternatives for solving battery issue. FC is used to generate electricity when PV and battery capacity do not meet electricity demand [7]. Fig. 2.2 represents the PV-battery-FC hybrid system configurations.

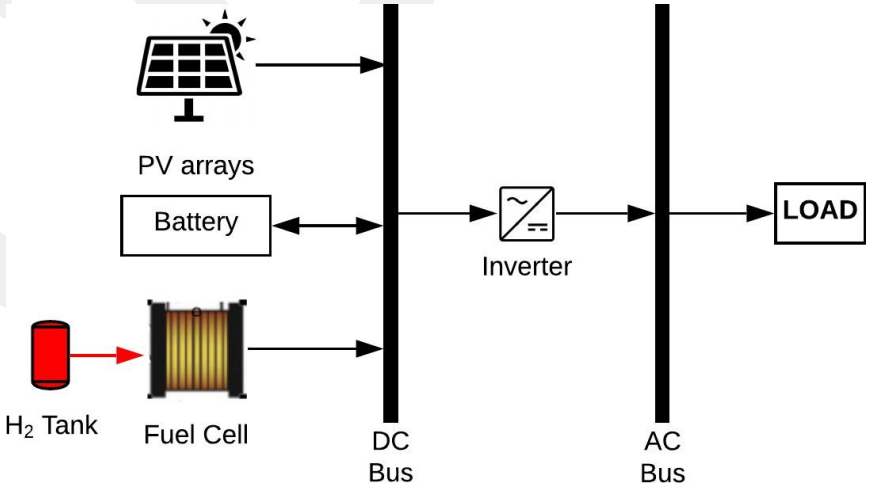

Figure 2.2: Schematic of a PV-battery-FC hybrid energy system

2.1.3. Photovoltaic-Electrolyzer-Fuel Cell Hybrid Energy System

To completely eliminate the battery problem, the best option is using electrolyzer in PV-FC hybrid energy system. The amount of energy is produced by PV cells. More than enough energy is used for operating of electrolyzer. Obtained H_2 from the electrolyzer is stored in a tank for use in the fuel cell. In this type of hybrid energy system, fuel cell operates during the hours when there is no sun. Thus, instant electrical energy is supplied from the fuel cell with H_2 drawn from the tank. The basic configuration of PV-electrolyzer-FC hybrid energy system is shown in Fig. 2.3. If the tank is chosen large enough, the hybrid energy system can store H_2 in the summer and be used for the electrical energy requirement in the winter. In addition, the using of PV-electrolyzer-FC hybrid energy system is an important alternative in rural areas in order to meet energy needs by itself [8].

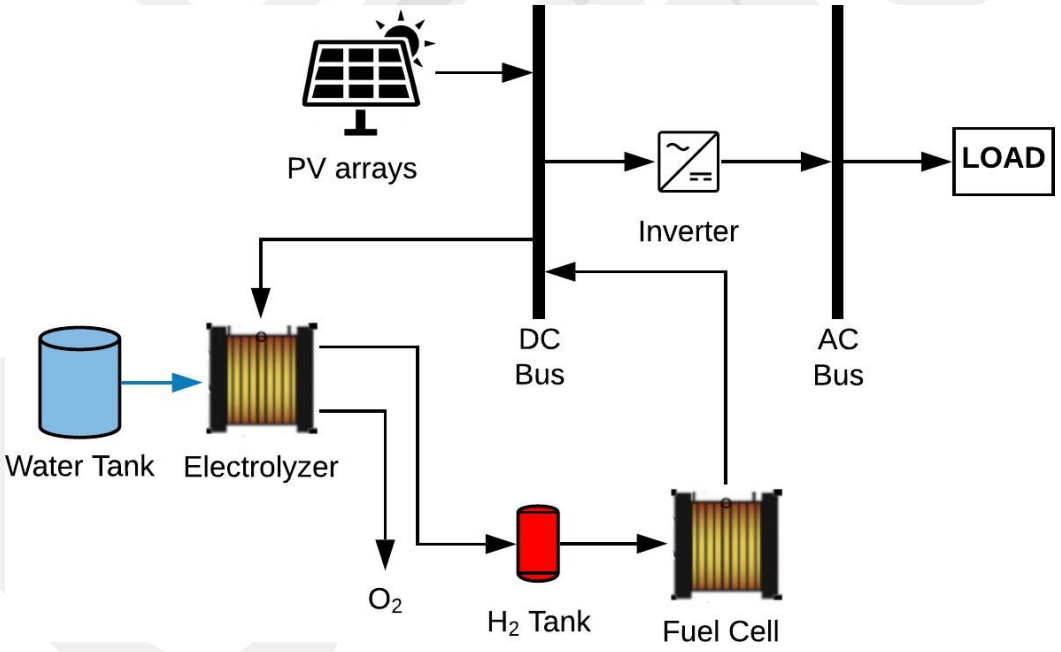

Figure 2.3: Schematic of a PV-electrolyzer-FC hybrid energy system

2.1.4. Photovoltaic-Electrolyzer-Fuel Cell Hybrid Energy System for Cogeneration Application

As the fuel cell can generate electricity, the thermal energy of fuel cell is also used in the cogeneration system. Heat demand of system is met with thermal energy emitted during electricity production [9]. Apart from the use of waste heat, removal of this heat is important for the safety and efficiency of the fuel cell [10]. While electricity generation is as PV-electrolyzer-FC hybrid energy system, heat cogeneration system is added to FC as shown in Fig. 2.4.

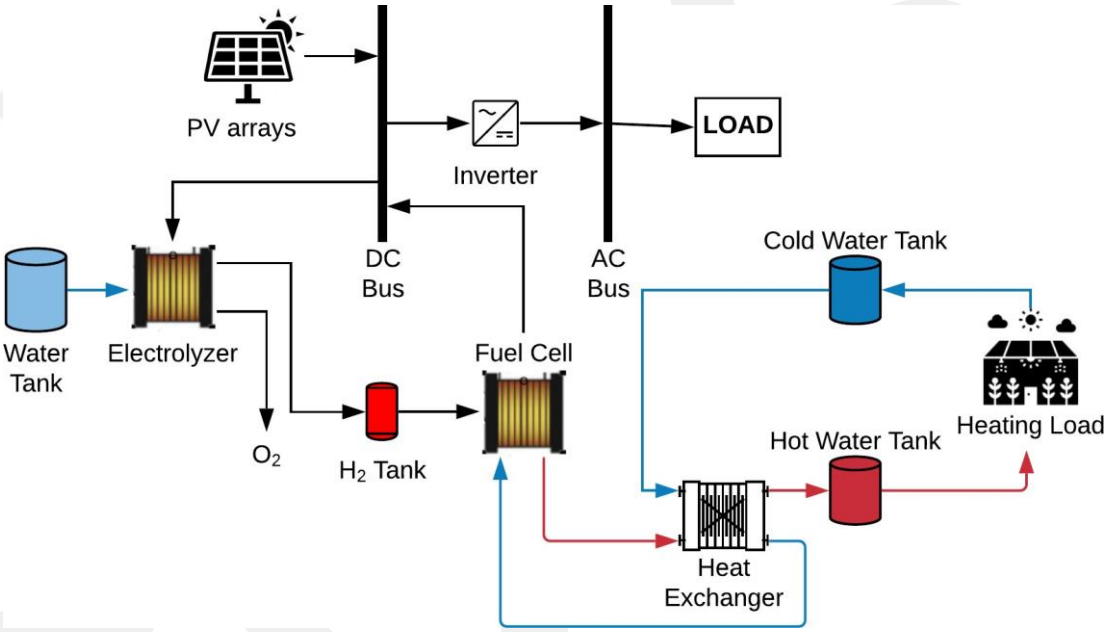

Figure 2.4: Schematic of a PV-electrolyzer-FC-cogeneration hybrid energy system

2.2. Description of PV-Electrolyzer-Fuel Cell Hybrid Energy System

2.2.1. Photovoltaic Generator

There are several thermodynamic pathways for converting solar energy into energy forms that can be used for human needs. Through the conversion of solar energy, heat,

kinetic energy, electric energy and chemical energy can generally provide [11]. There are two main ways of using solar energy to generate electricity. It can be transformed directly into electricity using PV or indirectly using solar collector which converts solar energy into heat energy so that it can be used in thermal power plants to generate electrical energy [12][13].

2.2.1.1. General Description of a Photovoltaic Cell

PV cells that consist of semi conductive materials can convert sunlight into electricity directly [14]. After the semiconductor *p-n* junction is formed, photons coming from the sun's rays break off electrons which are in *n*-type then they move towards the *p*-type. This case continues until load balance occurs on both sides. The lack of electrons (holes) and the excess of negative charge lead to the formation of an electric field on both sides of the junction. The photons of the light flux that absorbed by semiconductor form electron-hole pairs. As a result, during the flow the generation of electricity occurs as Figure 2.5.

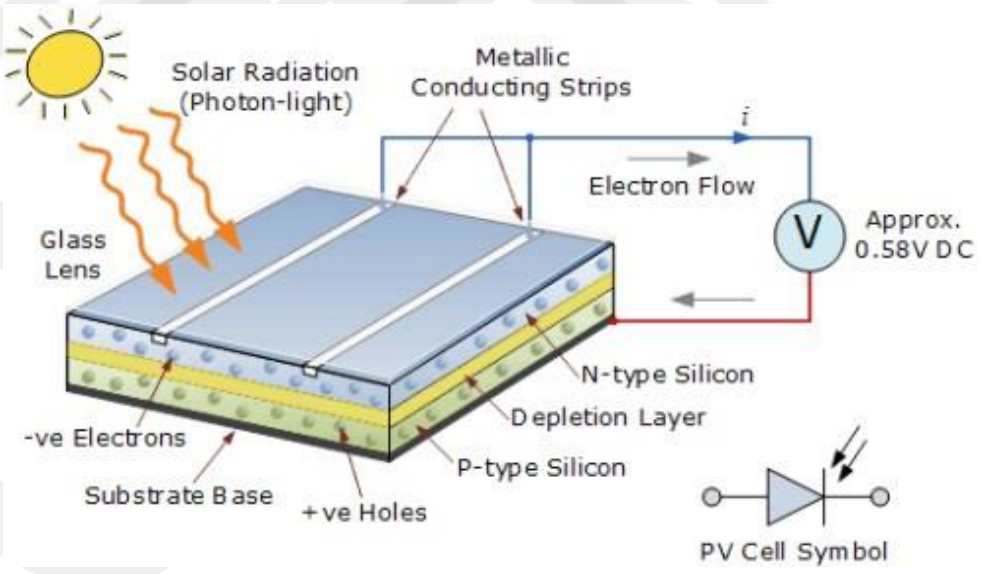

Figure 2.5: Cross section and working principle of PV cell [15]

It is possible to handle three types of PV cells; monocrystalline, polycrystalline, thin film and flexible.

Monocrystalline PV cells; consist of highly efficient monocrystalline cells. It takes up less space than polycrystalline which produces the same power. Since high technology is used during its production, the production time takes longer. It is called as ”mono” because only high purity crystal is used in its structure. Monocrystalline PV cells are long-lasting systems and their efficiency is around 24% [16].

Polycrystalline PV cells; although production equipment is easily accessible, energy efficiency is lower than monocrystalline solar cells. It is not produced in monocrystalline purity and is called as polycrystalline due to its heterogeneous structure. Their efficiency is around 16%.

Thin Film PV cells; are absorbing solar rays. Their efficiency is lower compered to crystal PV cells. They need large areas to produce high power due to their low efficiency. The approximate efficiency of thin film PV cells is around 7% [17].

Flexible PV cells; unlike traditional solar panel technology, they have been developed especially for roof applications. They are really flexible, unbreakable, very durable and easy to carry and apply. They do not need any construction or profile for their installation [18].

2.2.1.2. I-V Characteristics of a PV Cell

The equivalent circuit of PV cell is shown in Figure 2.6.

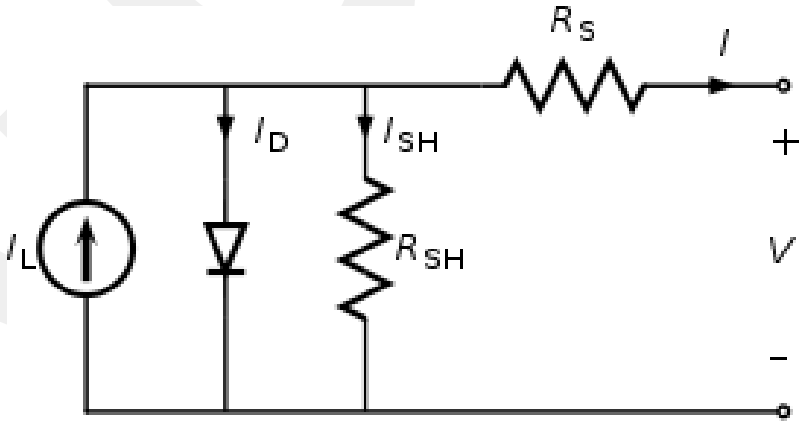

Figure 2.6: The equivalent circuit of PV cell

The current produced by PV cell is found as follows;

$$I = I_L - I_D - I_{SH} \tag{2.1}$$

Where; I = cell terminal current,

I_L = photogenerated current,

I_D = diode current,

I_{SH} = shunt current.

The diode current is described by the Shockley Equation 2.2 [19];

$$I_D = I_o \left[exp \frac{q(V+IR_s)}{kT_{cell}} - 1 \right] \tag{2.2}$$

Where; I_D = the net current flowing though the diode,

I_0 = reverse saturation current,

V = applied voltage,

I = cell terminal current,

R_S = series resistance,

q = magnitude of electronic charge (1.6×10^{-19}C),

k = Boltzmann's constant (1.38×10^{-23} J/K)

T_{cell} = absolute temperature of cell in Kelvin.

The cell terminal current is represented as [20];

$$I = I_L - I_0 \left[exp \frac{q(V+IR_s)}{kT} - 1 \right] - \frac{V+IR_s}{R_{SH}} \tag{2.3}$$

The typical I-V current described by Equation 2.3 is shown in Figure 2.7.

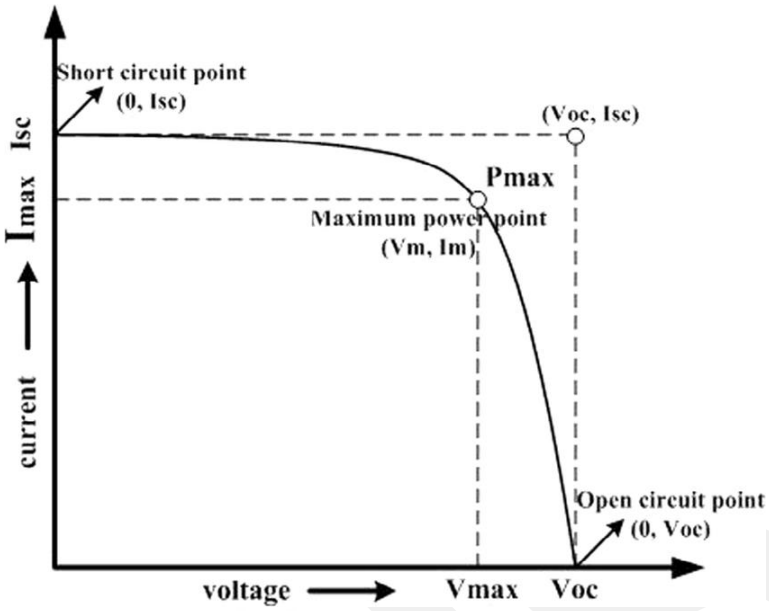

Figure 2.7: I-V characteristic of PV cell [21]

The PV cells behavior short-circuit at low voltages, so the current is approximately equal to short-circuit current (I_{SC}). With increasing voltage more than the maximum, the current starts to drop to zero exponentially. Maximum power point contains the maximum current and voltage at which the photovoltaic cell will operate at the highest efficiency.

2.2.2. Electrolyzer

Electrolysis is known as the simplest and efficiently method for water splitting to produce H_2. Electrolysis devices are called as electrolyzer. In electrolyzer, two electrodes (one with positively charged and the other with negatively charged) electrolyte placed in water solution. When the direct current voltage applied to electrolysis cell, water will decompose into H_2 gas at the cathode and O_2 gas at the anode. The reaction is endothermic [22]. For electrolysis of water, at normal pressure and temperature, 1.23 Volts will be enough ideally. Due to slow reaction and other reasons, higher voltage is used in electrolysis process. Since the H_2 production rate is proportional to the actual current intensity, high current densities are preferred for economic reasons. Therefore, in practice, the voltage applied per cell to separate water is usually around 2 volts.

2.2.2.1.Types of Water Electrolyzer

Alkaline, proton exchange membrane (PEM) and solid oxide electrolysis cells (SOEC) are commonly used electrolysis technologies. Typical specifications of these electrolyzers are shown in Table 2.1 [23]. The most important parameters are current density and efficiency.

In alkaline and SOEC electrolyzer, water is supplied from cathode side and it is split into H_2 and hydroxide ions (OH^-) which turns to anode side in order to from O_2. In PEM electrolyzer, water is split into O_2 gas, H_2 ions and electrons.

Table 2.1: Typical specifications of alkaline, PEM and SOE electrolyzers

Specification	**Alkaline**	**PEM**	**SOE**
Technology maturity	State of the art	Demonstration	R&D
Cell temperature, ^oC	60-80	50-80	900-1000
Cell pressure, bar	<30	<30	<30
Current density, A/cm^2	0.2-0.4	0.6-2.0	0.3-1.0
Cell voltage, V	1.8-2.4	1.8-2.2	0.95-1.3
Power density, W/cm^2	Up to 1.0	Up to 4.4	-
Voltage efficiency, %	62-82	67-82	81-86
Specific system energy consumption, kWh/Nm^3	4.5-7.0	4.5-7.5	2.5-3.5
H_2 production, Nm^3/hr	<760	<30	-
Stack lifetime, hr	<90000	<20000	<40000
System lifetime, yr	20-30	10-20	-
H_2 purity, %	>99.8	99.999	-
Cold start up time, min	15	<15	<60

2.2.2.2.PEM Type Water Electrolyzer and I-V Characteristics

In PEM electrolyzer, water is supplied from anode side. Water decomposes into O_2 gas, H_2 ions and electrons in the anode catalyst layer. As O_2 gas is taken out of the cell, H_2 ions (H^+) pass to the cathode through the electrolyte. Electrons on the external circuit passes to the cathode and combine with H^+ in the cathode catalyst layer and form H_2 gas. Thus, the electrolysis process is completed. The anode, cathode and total reaction that takes place during the production of H_2 and O_2 in PEM electrolyzer are as follows.

Anode reaction;

$$2H_2O \rightarrow O_2 + 4H^+ + 4e^- \quad (2.4)$$

Cathode reaction;

$$4H^+ + 4e^- \rightarrow 2H_2 \quad (2.5)$$

Overall cell reaction;

$$H_2O \rightarrow H_2 + \frac{1}{2}O_2 \quad (2.6)$$

Figure 2.8 shows the I-V characteristic of PEM electrolyzer. i.R_A is ohmic losses within the cell and its components where R_A is specific ohmic resistance.

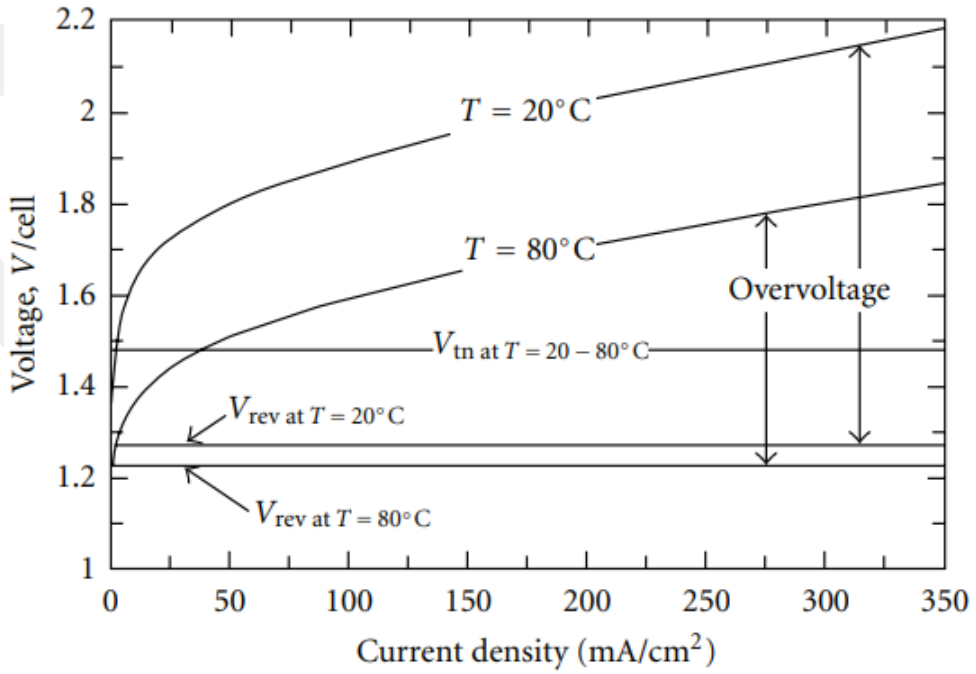

Figure 2.8: I-V characteristic of PEM electrolyzer [24]

2.2.3. H_2 Storage

Storability is the most important feature of H_2 and it must be stored in efficient and reliable for both fixed and portable applications. Three different methods can be mentioned about the storage of H_2. These are as pressurized gas, as liquid and as in the form of metal hybrid.

2.2.3.1.H_2 Storage as a Gas

The most basic and old technique of storage H_2 is pressurized tanks in gaseous state. Pressured tanks are produced in various sizes and pressures. The most common storage method is alloy steel tank at 200 bar pressure in industry and laboratory. Tanks should be durable for high pressure and also lightweight that is challenging in terms of tank design.

In storage as a gas, a method of increasing low volumetric density is stored as a liquid with low temperature such as liquid nitrogen temperature or cooling at -253 ^{O}C. But the required energy for liquefaction cannot be underestimated, it is approximately 1/4 of energy to be supplied from H_2. Ensuring the safety of pressurized tanks should be done carefully. A fuel leak can cause huge damage.

2.2.3.2.H_2 Storage as a Liquid

The most common storage method in large quantities is as a liquid. In this method, H_2 gas is cooled to 20 ^{O}K and stored in large tanks. The important thing is that H_2 does not contact with air, therefore, firstly the air of the tank is swept with nitrogen and then H_2 is pressed. The tank is usually kept at low pressures approximately 3 bar. The inconvenient part of this method is the liquefaction of H_2. It is compressed and cooled to 78 ^{O}K. Then it is inserted into a turbine and the temperature are also decreased. In addition, some changes are made at the atomic level [25].

2.2.3.3.H_2 Storage in Metal Hybrids

In this method, H_2 combines to form a metal hybrid and is heated if needed provided that they are separated and used. H_2 in unit volume can be stored more than pure liquid H_2 thanks to this method. This is because metal molecules are much closer than H_2

molecules and is taking H_2 molecules between them.

H_2 begins to be given to the tank which contains metal to react first. This reaction changes direction depending on pressure and temperature, and may be endothermic or exothermic, depending on the type of metal. When the reaction is over, by means, when all the metal is compounded with H_2, the pressure will increase. It signals to stop feeding H_2. All processes are repeated when tank is completely empty. A system is gotten that can load and unload hundreds of times. Also this method is successful for security in low pressure. The biggest disadvantages is that it takes a lot of time to reload the tank [26].

2.2.4. Fuel Cell

In the search for new energy sources to meet the increasing energy demand in the world, fuel cells are one of the most important approaches used in clean energy production and which are expected to be widely used in the future. Fuel cells are device that convert chemical energy into electrical and heat energy without combustion [27]. Fuel cells continue to generate uninterrupted electricity as long as fuel is supplied. At the end of the process, pure water vapor and heat are generated as waste.

2.2.4.1.History of the Fuel Cell

The fuel cell was first found in 1839 by William Grove, who was also a judge and an amateur scientist. Grove succeeded in producing H_2 and O_2 in a system consisting of two platinum electrodes immersed in dilute sulfuric acid ($H_2S\,O_4$) solution. In the later years, Grove managed to produce more electric currents by combining fifty of the previous system. The term of Fuel Cell was named by Ludwing Mond and Charles Longer, who carried out studies in this field in 1889. The first successful fuel cell construction and implementation was in 1932 by Francis Bacon [28]. Between 1959 and 1960, NASA did serious work in this field. 200 researches were made in the field of fuel cell for use in space vehicles and eventually produced fuel cell that generates electricity and water vapor to meet their requirements. This fuel cell has been used in spacecraft, such as the Apollo Space Ship and Space Shuttle [29]. While the first fuel cells were produced for the Apollo space program and have been used in space programs and also transportation and small electric productions.

2.2.4.2.Working Principle of Fuel Cell

H_2 which is the main fuel of Fuel Cell reacts with air or O_2. After the reaction, electricity, heat and pure water are produced. H_2 fuel is supplied by the anode side of the fuel cell and air or O_2 is supplied by the cathode side. On the anode side of H_2, it decomposes into positive and negative ions. Positive ions reach the cathode side by the help of electrolyte, which allows only positively charged ions to pass. The electrons remaining at the anode end tend to reunite with positively charged ions and flow through the cathode side by an external circuit. This electron flow in the external circuit generates electricity. The electrons passing to the cathode side combine with positive ions and air and pure water is formed [30].

2.2.4.3.Types of the Fuel Cell

Fuel cells are classified according to the used electrolyte and working temperature [31]. There are several types of fuel cells as shown in Figure 2.9.

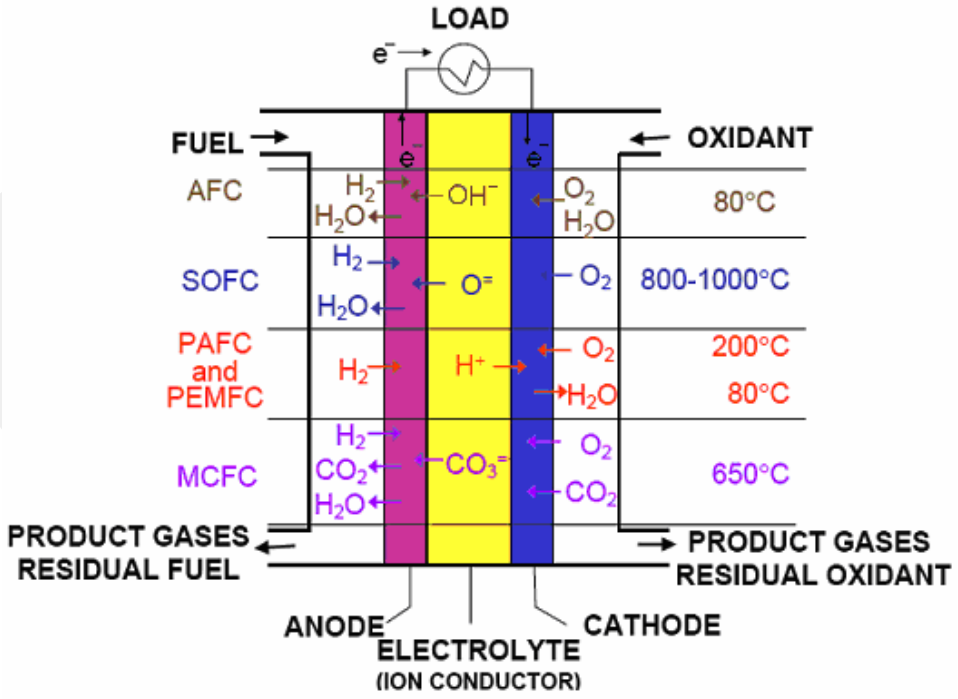

Figure 2.9: Types of the Fuel Cell [32]

Solid Oxide Fuel Cell (SOFC)

The SOFC operates at high temperatures and has good performance. Since the operating temperature is 900 ^{O}C-1000 ^{O}C, materials of SOFC electrolyte are made of solid oxide ceramics such as yttrium oxide or zirconium [33]. There are some disadvantages such as high operating temperature, slow start-up, low performance under 800 ^{O}C. It is used in industrial areas and electricity production centers.

Molten Carbonate Fuel Cells (MCFC)

MCFC is capable of operating at temperature as high as 600 ^{O}C-650 ^{O}C. For the electrolyte, mixture of lithium and potassium carbonates are generally used, which has a melting temperature around 550 ^{O}C. This mixture is usually impregnated into porous ceramic matrix made of lithium aluminate ($LiAlO_2$) [34]. If the operating temperature is higher than 650 ^{O}C, durable materials should be used for preventing corrosion. Corrosion and molten electrolyte are the disadvantages of MCFC's [35].

Alkaline Fuel Cell (AFC)

Concentrated solution of potassium hydroxide (KOH) is used for electrolyte in AFC's. Hydroxyl ions are transformed from the cathode to the anode with the help of this solution. The operating temperature of the AFCs is higher than 60 ^{O}C and lower than 120 ^{O}C. In addition to generate electricity, AFC's produce potable water and for this reason, they are used in various space applications by NASA. The main disadvantages of AFC's are that, H_2 and oxidation must be very pure. Even a small amount of carbon dioxide (CO_2) is very harmful for electrolyte. CO_2 reacts with electrolyte and causes poisoning. This affects fuel cell performance negatively [36].

Phosphoric Acid Fuel Cell (PAFC)

Phosphoric acid is used as the electrolyte. PAFC consists of a porous matrix surrounded by porous carbon electrodes, which holds the liquid phosphoric acid electrolyte. PAFC system operates at a temperature of about 200 ^{O}C because phosphoric acid has low conductivity at low temperatures. The most progressive type

of fuel cells is PAFC which is the first commercially available application [37].

Proton Exchange Membrane Fuel Cell (PEMFC)

PEMFC's contain two electrodes; anode and cathode. These electrodes they are separated from each other by polymer electrolyte membrane. Both electrode layers also covered by a thin layer of catalyst. PEMFC's is the most promising power generation device for automotive, portable application, off-grid and on-grid power plant. Also PEMFC's are the most popular type of fuel cells due to their advantages which are high power intensity, high efficiency, quick start-up, low operation temperatures, long- life, portable water as product, easy design and dimension flexibility, fast response to changing loads during operation [38]. Besides its advantages, some disadvantages can be listed as; electrolyte (membrane) cost, sensitivity to carbon monoxide (CO), limited structural strength properties and need to use lots of catalysts [39].

2.2.4.4.PEMFC Operation

The schematic diagram of PEMFC is shown in Figure 2.10. PEMFC consists of anode, cathode, electrolyte layer and gas channel collectors. H_2 and O_2 pass through the gas channels and reach the anode and cathode, respectively. These gases reach the proton permeable membrane after passing through the diffusion layer. In the anode side, H_2 fuel is catalyzed and separated into protons and electrons. H_2 protons pass through the polymer electrolyte membrane and combine with O_2 in the cathode side. After the combination, water is obtained. H_2 electrons passing from anode to cathode produce electrical energy [40].

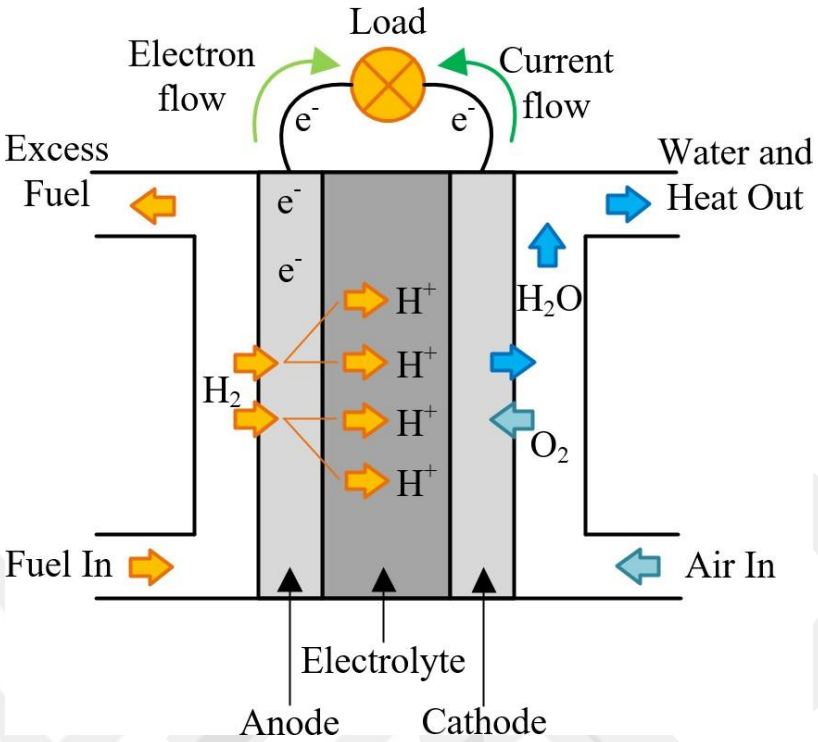

Figure 2.10: Schematic Operation Diagram of PEMFC [41]

The reactions of PEMFC's process are as follows;

Anode reaction is given in Equation 2.7;

$$H_2 \rightarrow 2H^+ + 2e^- \tag{2.7}$$

Cathode reaction is given in Equation 2.8;

$$\frac{1}{2}O_2 + 2H^+ + 2e^- \rightarrow H_2O \tag{2.8}$$

Overall cell reaction is given in Equation 2.9;

$$H_2 + \frac{1}{2}O_2 \rightarrow H_2O + Energy \tag{2.9}$$

2.2.4.5. PEMFC Characteristics

The PEMFC energy potential in Equation 2.10 can be found with Gibbs free energy as below [42];

$$E = \frac{-\Delta G}{nF} \tag{2.10}$$

At the standard condition (T=25 $^{\circ}$C, P=1 atm), PEMFC potential is equal to E=1.23 V theoretically. However, the PEMFC potential is less than the theoretical potential due to some losses. PEMFC electrical losses can be investigated three main categories; the activation polarization losses (V_{act}), the ohmic (resistive) losses (V_{ohm}) and the concentration polarization losses (V_{conc}) [43].

$$V_{FC} = E - V_{act} - V_{ohm} - V_{conc} \tag{2.11}$$

The activation loss is voltage drop according to activation of anode and cathode and occurs in the low current region. Low current density change in cathode activation is the main reason for this loss. The resistance of the electrolyte liquid to ion transfer creates ohmic losses. These resistors consist of ionic (R_{ion}) and electronic resistors (R_{elc}). While ionic resistance refers to the ion-permeability of the electrolyte, the electronic resistance refers to the total electrical resistance, including the resistance of all other elements, such as the catalyst surface, the gas diffusion surface. Diffusion flow and mass transfer occur at micro level on diffusion surface and catalyst surface. Electrochemical reactions occurring on the catalyst surface cause the concentration of H_2 to decrease and concentration losses to occur [44]. It is called as concentration polarization loss. General polarization curve of PEMFC is shown in Figure 2.11.

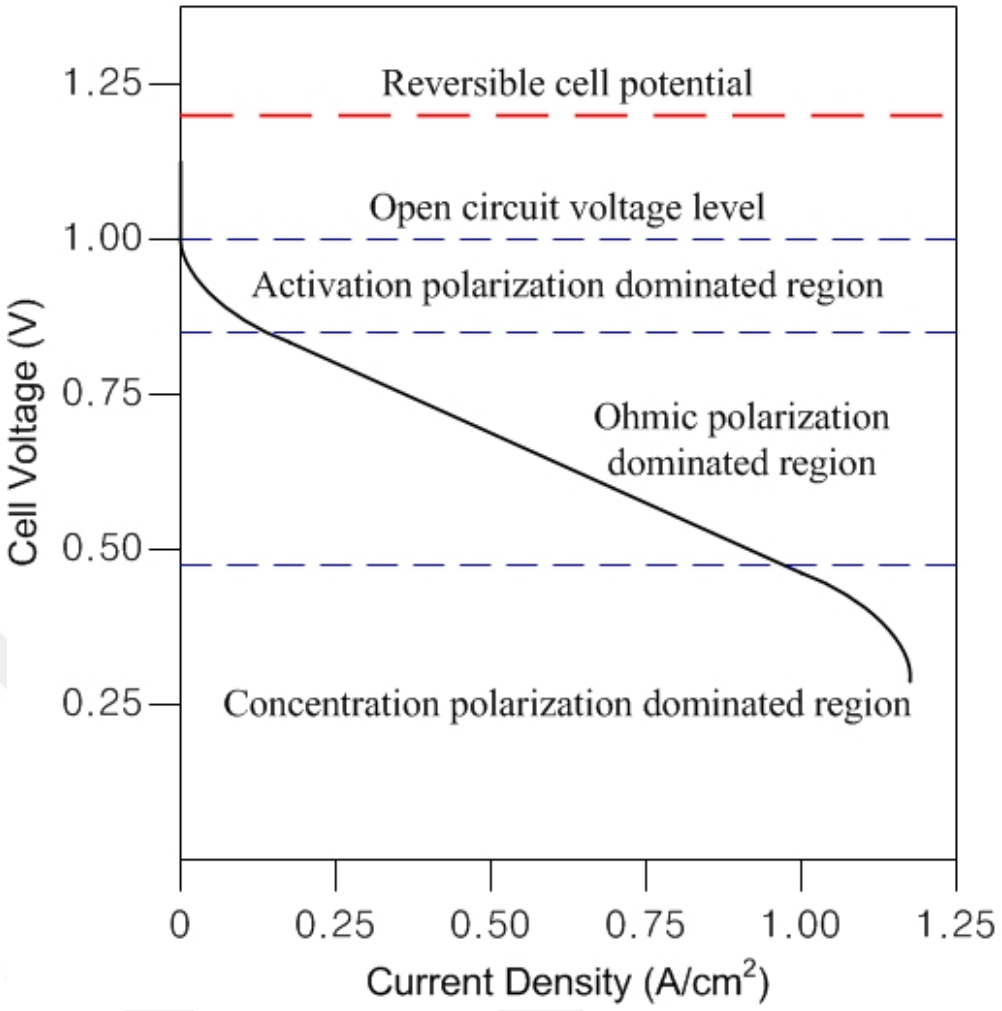

Figure 2.11: General polarization curve of PEMFC [45]

2.2.5. CHP System

CHP system is the production of energy from the same system in both electricity and heat forms. Gas turbine or engine which generate electricity can convert 30-40% of energy to electricity. If this system is used in the form of CHP system, most of the heat energy to be expelled from the system can be converted into usable energy and the total energy can be evaluated between 70-90%. It means that, CHP system increases the efficiency of the system. The heat energy can be used for space heating, hot water or industrial processes. Energy savings, which will be achieved by meeting the electrical energy and thermal energy required for both industrial and residential

heating from the same source, will reduce environmental pollution and dependence on another sources. Therefore; CHP system, which is the providing of electricity and heat energy from the same source, is required [46][47].

2.3. Motivation of This Study

The summaries of some studies on hybrid energy systems are as follows.

Hybrid power generation systems can be made with many combinations of different energy sources and storage devices. Solar and wind energy are among the most widely used renewable energy sources in a hybrid power generation system. In applications from the network independent wind and solar power generation systems are often operated with gas turbines, diesel generators, fuel cells and battery packs. With it energy continuity and system performance are increased [48].

Eroglu et al. worked on the application of a hybrid power system consisting of PV-wind and fuel cell on a mobile home. In this study, where solar and wind energy was used as the first source, the fuel cell was evaluated as a secondary source. In mobile home energy application, H_2 is obtained by electrolyzer and compressed with high pressure and stored in H_2 tanks. In cases where wind and solar energy are insufficient, H_2 energy is burned in the fuel cell and electrical energy is obtained to ensure continuity. PV (800W), a wind turbine (1kW) and a fuel cell (2kW) were used in this hybrid energy system to generate 3.8 kW power [49].

Ghenai et al. designed PV-Fuel cell-electrolyzer hybrid energy system to supply energy demand of 150 houses which was about 4500 kWh/day. 52% of power production came from PV and 48% of it came from the fuel cell. LCOE of the hybrid system was 145$/MWh [50].

A PV-Fuel Cell-electrolyzer hybrid energy system used in stand-alone application has been studied by Lajnef et al. This hybrid energy system solved the energy storage problem, since electrical energy was stored in the form of H_2. MATLAB/Simulink and SimPower- System were used for modeling and simulation [51].

Özgirgin et all described a hybrid energy system for house-hold micro co-generation applications. The hybrid energy system consisted of PV (33.6 m^2), PEMFC (1200 W),

batteries, PEM electrolyzer (4700 W), plate type HEX. While generated electricity was storing at batteries, the released heat from PEMFC was used for heating of the house [52] .

Isa et all proved that a hybrid system with cogeneration was feasible for a hospital in Malaysia. The proposed hybrid system consisted of PV (120 kW), batteries, converter (40 kW), diesel generator (5 kW), fuel cell (100 kW), H_2 tank (80 kg). Economic parameters were simulated in HOMER software and the lowest LCOE was \$0.0841/kWh [53].

A hybrid system was designed to meet the electricity requirement of 90 m^2 floriculture greenhouse by Ganguly et al. The hybrid system contained 51×75 W_p PV cells, 3.3 kW electrolyzer and 2×480 W PEMFC [54].

There are lots of studies in the literature about the PV-electrolyzer-PEMFC hybrid energy system. The motivation of this study was that, electricity and heat demand of greenhouse was met by PV- electrolyzer-PEMFC hybrid energy system with cogeneration. After calculating the power of PEMFC, which would meet the electrical needs of the greenhouse, 2.4 kW, the design of the electrolyzer that would meet the H_2 requirement of the PEMFC was designed. PV cells were used for the operation of the electrolyzer and the number of these cells was determined. The amount of produced H_2 was used for PEMFC, the excess was stored in the H_2 tanks for use future. Taking advantage of the operating temperature of the fuel cell, waste heat was used to heat the greenhouse. All calculations were made in MATLAB/Simulink.

CHAPTER 3

3. EXPERIMENTAL STUDIES

3.1.Present System and Design of Proposed Hybrid Energy System

In the present system of greenhouse, while electricity is pulled from the grid, the greenhouse is heated by heating system with coal furnace. A fluid is heated and circulating it in a closed system. In addition to being expensive in the first construction of this heating system, operating cost are also high. Coal energy is converted into heat energy in the coal furnace. With the heat obtained, hot water or steam is produced in the boiler. The pump and motor are used to send the hot water or steam to the system in the greenhouse, and various materials and parts are used to control their operation. Approximately 1891 kW of electricity is consumed annually and 500 tons of coal is burned for heating.

In today's world, where energy prices are high, greenhouse heating costs increase and the cost of the products grown increases. For this reason, the cheapest energy sources are used for meeting energy demand and heating the greenhouse. Due to high energy costs obtained from conventional energy sources, new and renewable energy sources have been getting importance for greenhouse heating purposes. It is a priority requirement to use natural energy sources instead of fossil energy sources in order to protect today's energy existence and prevent environmental pollution.

Since customer electric bills shows the changes of consumed electricity, amount of consumption can be investigated easily [55]. Using existing energy bill data can reduce the effects of input uncertainty and result in more reliable output [56]. In this thesis, the amount of greenhouse electricity consumption data was taken from its electric bill and it is shown in Figure 3.1. It is understood that, the maximum electricity consumption of greenhouse is approximately 325 kW in August and the minimum is approximately 75 kW in December.

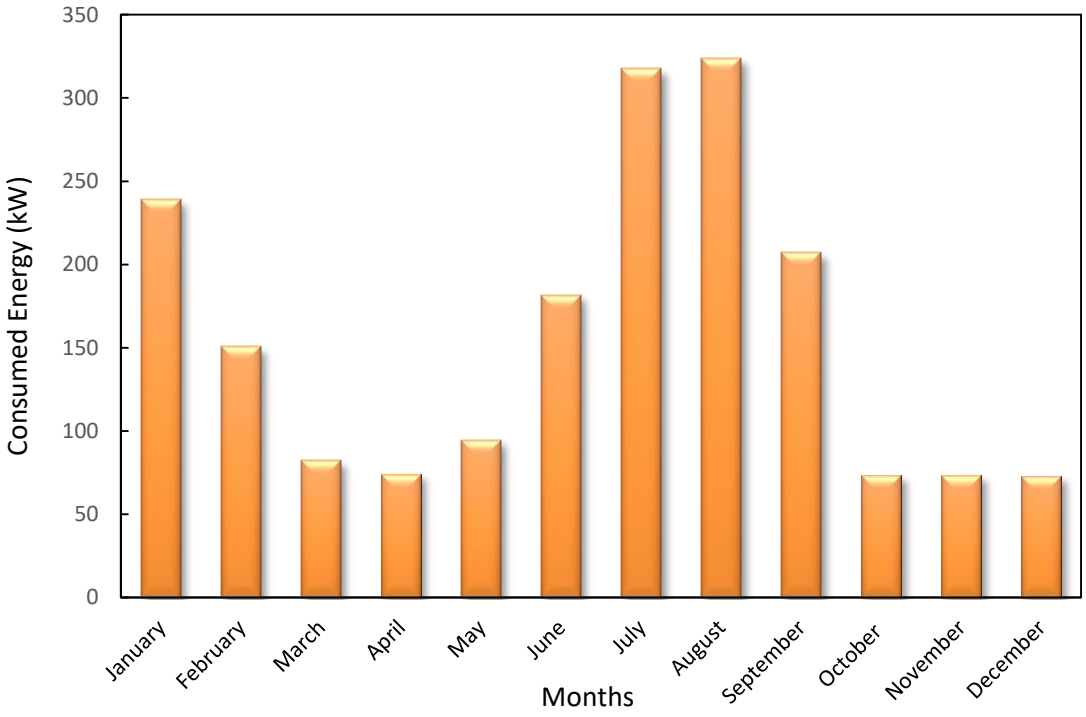

Figure 3.1: The amount of greenhouse energy consumption monthly

When the power system is installed, it must be enough to meet the maximum energy demand. According to energy demand of greenhouse, it was anticipated that, 2 kW PEMFC operating 5 hours a day would be sufficient but it was designed 2.4 kW.The aim of that, approximately 20 % of designed PEMFC power is consumed by auxiliary equipment.

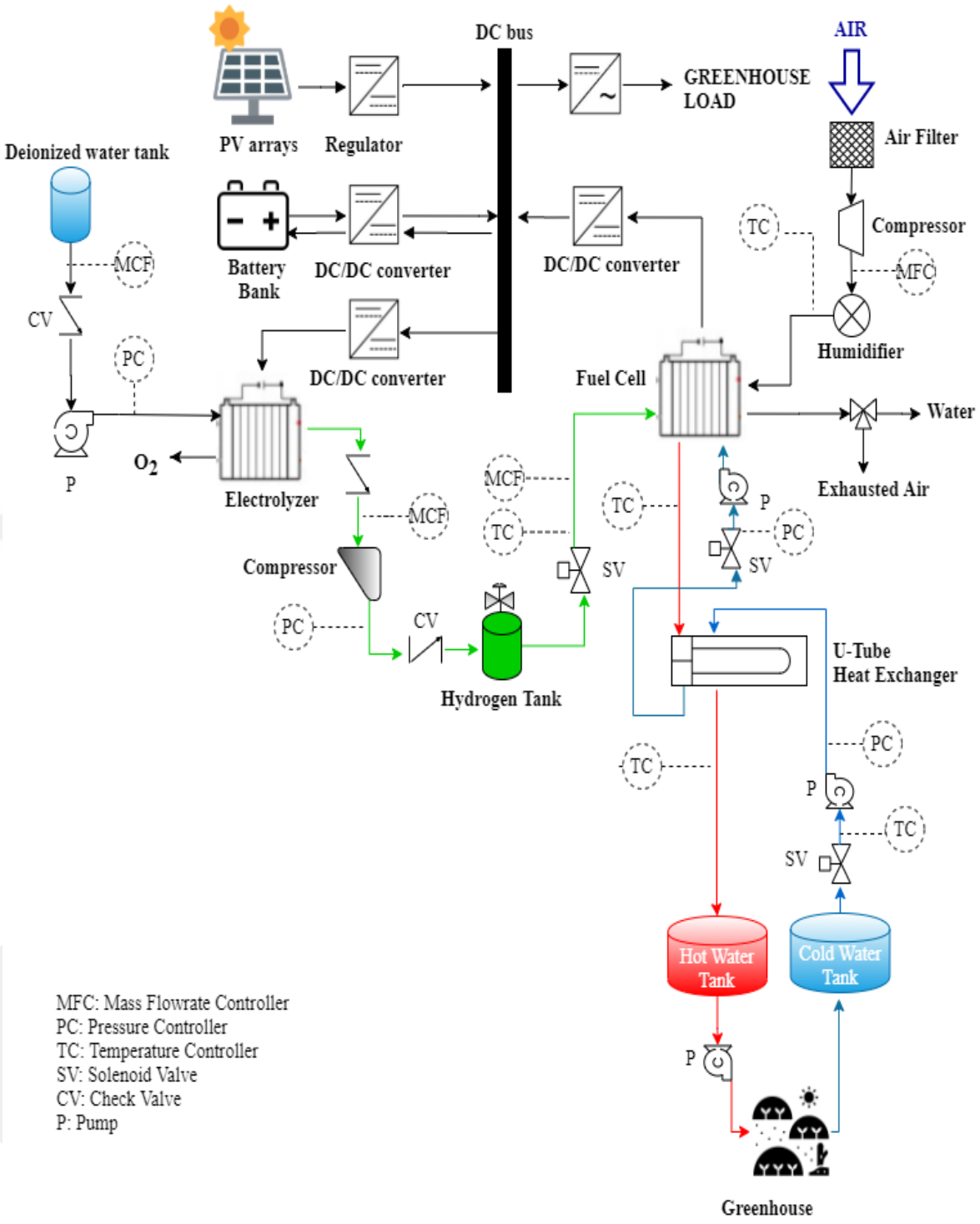

Figure 3.2: Proposed hybrid energy system design

PV-electrolyzer-PEMFC-cogeneration hybrid energy system is given Figure 3.2. Electrolyzer uses electricity generating from PV arrays. The water to be separated comes from the deionized water tank and it is split H_2 and O_2. The produced H_2 is stored in the H_2 tank for PEMFC. The produced O_2 is released to the atmosphere and the O_2 requirement of PEMFC is supplied from the air. Air is filtered, humidified and fed to PEMFC with the help of a compressor. The produced H_2 was stored in storage tanks to be utilized by the PEMFC when the PV energy fail to supply the load demand.

The produced heat in PEMFC was removed from the PEMFC by a cooling system to operate PEMFC at a constant temperature [57]. Two water loops were used for CHP application and they were unmixed and pumped by means of the water pumps. The PEMFC cooling water flows through PEMFC cooling channels to remove heat produced from exothermic reaction. This exothermic reaction causes overheating problem that shortens the lifetime of PEMFC [58]. Then PEMFC cooling water was sent to the heat exchanger. The greenhouse water enters the heat exchanger from the other line and warms up and meets the hot water requirement. Thanks to this hybrid energy system, the electricity and heat demand of the greenhouse are met.

3.2.Components of the Proposed Hybrid Energy System

Proposed PV-electrolyzer-PEMFC-cogeneration hybrid energy system components are shown in Table 3.1. In addition to these, hybrid energy system contains 19330 L H_2 storage tank, U-tube heat exchanger, a regulator, three DC/DC converters, two compressors for air and H_2, a deionized water tank, two water tanks for hot and cold water, several pumps and valves.

Due to counter flow principle, a U-tube heat exchanger is commonly used and the heat transformation occurs in opposing directions between hot and cold flow. End of the transformation, heat recovery of almost 100% is achieved. So, U-tube heat exchanger provides a very high efficiency to the system. One of the most important features is that it is easy to clean.

Table 3.1: Proposed hybrid energy system components

Component	Parameter	Value
PV [59]	Type of cell	Monocrystalline
	Max power	360W
	Size	1956 mm×992 mm×40 mm
	Efficiency	21.5 %
PEM electrolyzer [60]	Membrane	Perflorosulfonic acid
	Cell area	200 cm^2
	Cell number	32
	Current density (at 1.5 V)	1 A/cm^2
	Efficiency	88%
PEMFC [61]	Electrolyte	Nafion 212
	Active area	150 cm^2
	Cell number	32
	Current density (at 0.6V)	1A/cm^2
	Design power	2400 W
	$\lambda_{anode}/\lambda_{cathode}$	1.0/2.5
	Working temperature	70 ^oC
	H_2 flow rate	36.52 slpm
	O_2 flow rate	38.04 slpm
Battery [62]	Nominal voltage	24 V
	Nominal current	150 Ah
	Depth of discharge (DoD)	85%

3.3.Optimal Design Strategy of the Proposed System

Optimal design strategy of the proposed system is shown in Figure 3.3. Before starting the design of the hybrid system, how much electrical energy will be sufficient for the greenhouse is calculated. The power of PEMFC is calculated ac- cording to electricity requirement. After finding the amount of H_2 to be consumed by PEMFC, the minimum power of electrolyzer ($P_{min,el}$) is found to meet H_2 demand. PV arrays produce electricity for operating electrolyzer and how many PV arrays used the system are calculated based on the $P_{min,el}$. The electricity produced by PV arrays changes due to

total solar radiation and ambient temperature.

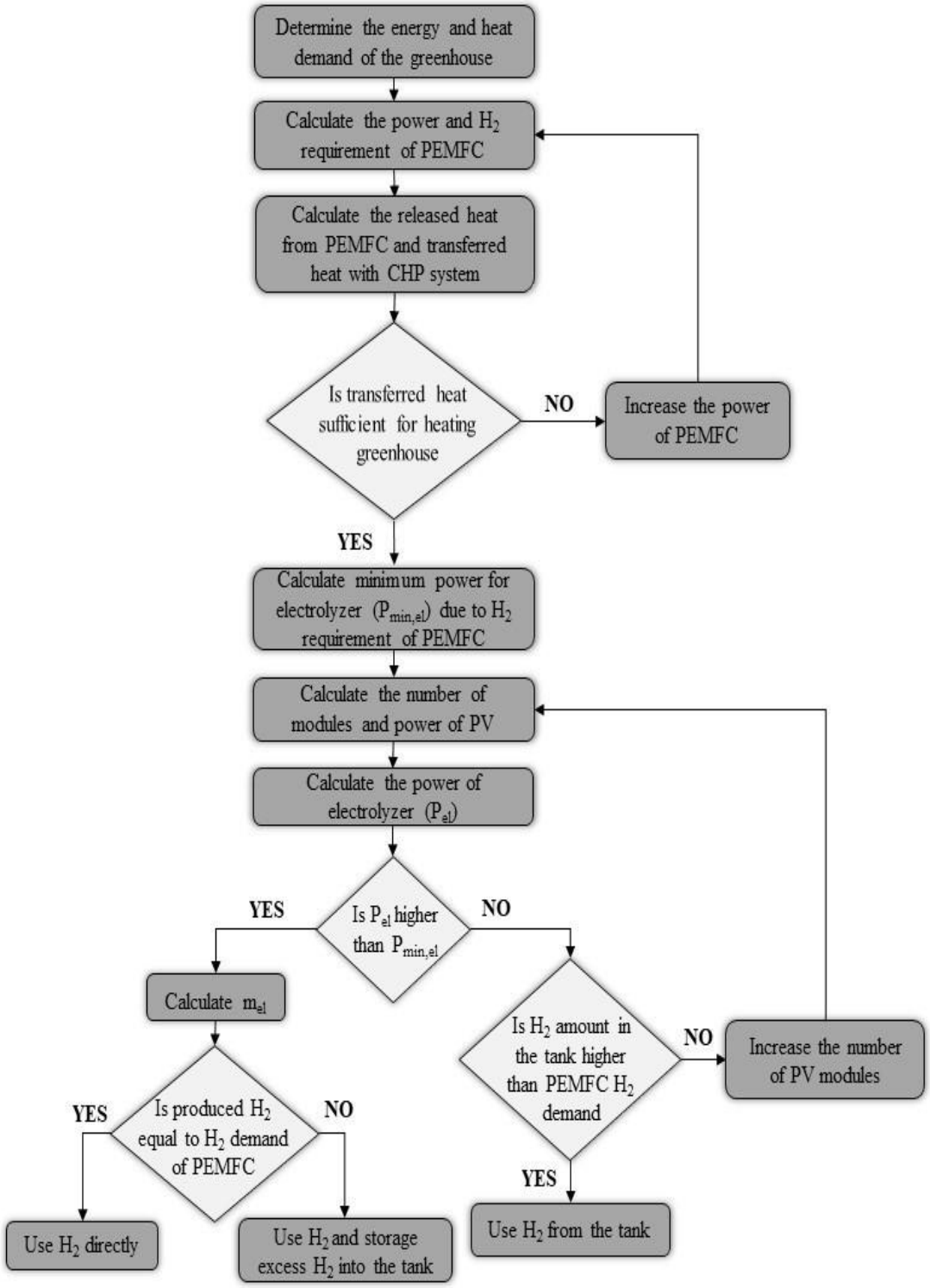

Figure 3.3: Optimal design strategy of the proposed system

If the generated electricity is equal or greater than the $P_{min,el}$, electrolyzer will start to produce H_2. If the produced electricity is smaller than $P_{min,el}$, the electrolyzer will not work and H_2 is used from the tank. Produced H_2 is used directly and the excess is stored in tank. On the other hand, the obtained heat while PEMFC is operating is used for greenhouse heating.

3.4.Design Calculation

3.4.1. Solar Calculation

This thesis was conducted for the Şanlıurfa, Turkey (37 N, 38E) [64], as shown in Figure 3.4.

Figure 3.4: Location of greenhouse and Şanlıurfa in Turkey [63]

The measured daily global irradiation and ambient temperature data were taken from Turkish State Meteorological Service for 365 days. Figure 3.5 shows the measured total solar radiation and Figure 3.6 shows the measured daily ambient temperature. These data were used for PV design calculations. When the data are examined, the maximum and the minimum solar irradiation were obtained 8.7 kWh/m^2 and 0.3 kWh/m^2, respectively. The highest and lowest temperature were 32°C on July, 3 and 3.9°C on December, 10.

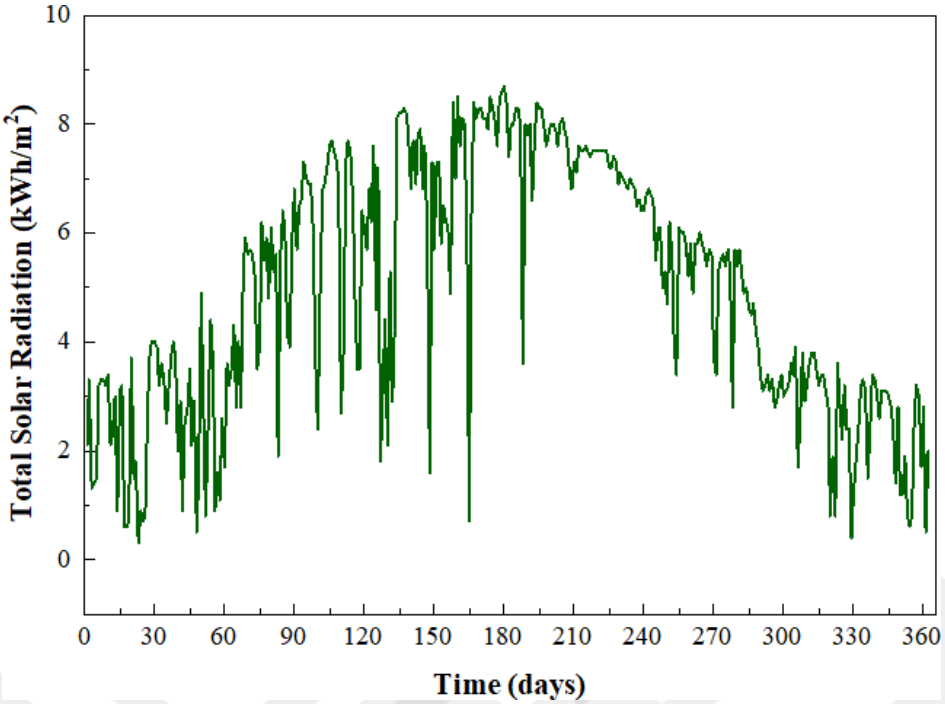

Figure 3.5: Measured Total Solar Radiation

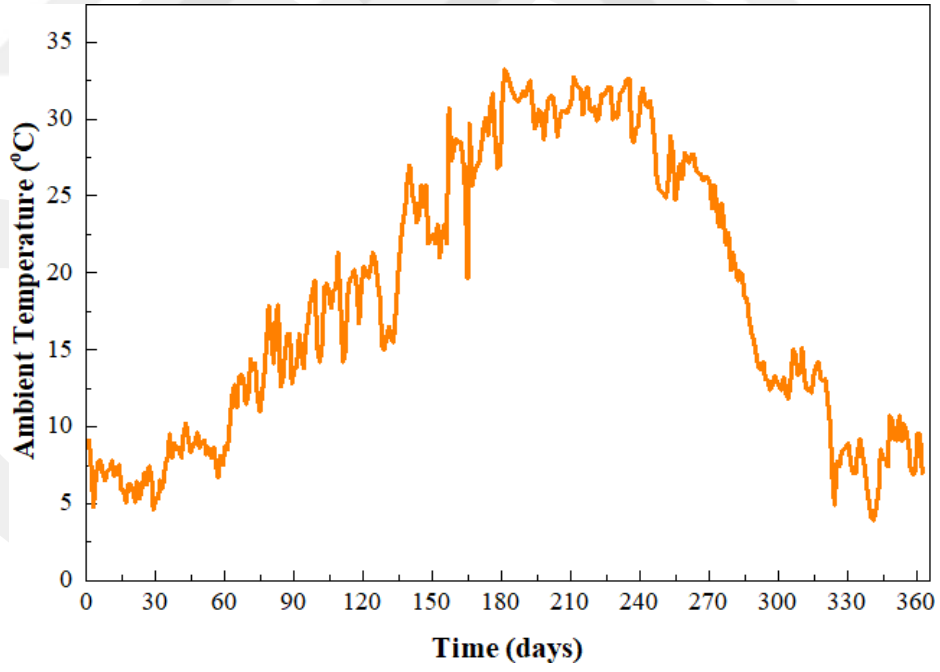

Figure 3.6: Measured Daily Ambient Temperature

The power of PV arrays was calculated according to Tebibel and Equation 3.1 gives it [65].

$$P_{PV} = N_{PV} \frac{G_I}{G_{I,ref}} \left[P_{PV,max} + \mu_p \left(T_{cell} - T_{c,ref}\right)\right] \quad (3.1)$$

Where N_{PV} refers the number of PV arrays, G_I and $G_{I,re\ f}$ are solar irradiance and the reference solar irradiation of PV, respectively. $P_{PV,max}$ is the maximum power of PV cell. $G_{I,ref}$ is 1 kW/m^2 and $P_{PV,max}$ is 0.38 kW, these values are the features of the selected PV array. The power thermal coefficient is represented by μ_p. $T_{c,ref}$ refers the PV cell temperature at standard conditions (25^{O}C). PV cell temperature (T_{cell}) can be calculated according to ambient temperature (T_a), G_I and nominal operating cell temperature (NOCT, 45^{O}C) by following equation:

$$T_{cell} = T_a + G_I \frac{NOCT - 20}{800} \quad (3.2)$$

3.4.2. Electrolyzer Calculation

Since consumed H_2 molar flowrate of PEMFC ($N_{H_2 PEMFC}$) is known, the cell number of PEM electrolyzer (N_{cell}) is calculated by Faraday's laws in Electrolysis from Equation 3.3 [66]:

$$N_{cell} = \frac{N_{H_2 PEMFC} \times n \times F}{i \times A} \times \frac{1}{\eta} \quad (3.3)$$

Where, n is the transferred electron number of H_2. F is Faraday constant. i, A and η refer to current density, cell area and efficiency of the PEM electrolyzer, respectively. These values are listed in Table 3.1.

The voltage of electrolyzer (V_{elec}) depends on the the cell voltage of electrolyzer (V_{cell}) and N_{cell}. The multiplying of the both gives the V_{elec} as following equation:

$$V_{elec} = V_{cell} \times N_{cell} \quad (3.4)$$

The minimum power of electrolyzer ($P_{el,min}$) is associated with electrolyzer voltage, current density and electrolyzer active area. Multiplying three gives $P_{el,min}$.

$$P_{el,min} = V_{elec} \times i \times A \quad (3.5)$$

H_2 molar flowrate produced by electrolyzer is calculated as below;

$$m_{el} = 1.43 \times 10^{-3} + 2.39 \times 10^{-2} P_{el} - 4.32 \times 10^{-5} P^2{}_{el} \quad (3.6)$$

Where P_{el} is the power of electrolyzer which changes with power of PV arrays and efficiency of DC generator.

$$P_{el} = P_{P\,V} \times \eta_{dc} \quad (3.7)$$

3.4.3. PEMFC Calculation

The consumed H_2 and O_2 or air concentration rate and the generated water mass flowrate are determined by Faraday's Law [28]:

$$\dot{m}_{H_2} = S_{H_2} \times \frac{i \times A}{2 \times F} \times N_{cell} \times M_{H_2} \quad (3.8)$$

$$\dot{m}_{O_2} = S_{O_2} \times \frac{i \times A}{4 \times F} \times N_{cell} \times M_{O_2} \quad (3.9)$$

$$\dot{m}_{air} = \frac{S_{O_2}}{r_{O_2}} \times \frac{i \times A}{4 \times F} \times N_{cell} \times M_{air} \quad (3.10)$$

$$\dot{m}_{H_2O} = \frac{i \times A}{4 \times F} \times N_{cell} \times M_{H_2O} \quad (3.11)$$

Where, S_{H_2} = Stoichiometric ratio of H_2, S_{O_2} = Stoichiometric ratio of O_2,

r_{O_2} = O_2 volume in air (21%),

i = Current density (A/cm^2),

A = Total active area of PEMFC (cm^2),

F = Faraday constant (96485 Cmol^{-1})),

N_{cell} = Cell number of PEMFC,

M_{H_2} = Mass of H_2 (g/mol),

M_{O_2} = Mass of O_2 (g/mol),

M_{air} = Mass of air (g/mol),

M_{H_2O} = Mass of H_2O (g/mol).

By calculating the energy balance of the fuel cell, waste heat (Q) is found in Equation 3.12. This amount of waste heat is used for heating greenhouse.

$$\sum \dot{E}_{mass,in} - \sum \dot{E}_{mass,out} + Q - \dot{W}_{net} = 0 \quad (3.12)$$

Where, total enthalpy of inlet gasses and total enthalpy of outlet gasses are represented $\dot{E}_{mass,in}$ and $\dot{E}_{mass,out}$, respectively. $\dot{W}_{net}$ is net power of PEMFC.

3.4.4. H_2 Storage Calculation

The volume, pressure, temperature and quantity of the gas which are the basic parameters determine the physical behavior of the gases. According to Avogadro's Law, when pressure and temperature are constant, the volume of a gas (V) changes in proportion to the mole number of gas (n) and the volume is calculated in below [67]:

$$PV = nRT \quad (3.13)$$

Where, P is pressure, T is temperature and R is Regnault constant (8.314 kJ/kmol.K). Equation 3.13 is called as ideal gas equation. Real gases do not fully comply with ideal gas law. From the law deviations are particularly important at high pressures and low temperatures, especially when a gas is at the condensation point. Real gases deviate from the ideal gas law because molecules interact with each other. Propellant between molecules forces help to expand and attractive forces help to compression. The compressibility factor (Z) is association with reduced pressure (P_R) and reduced temperature (T_R) [68]. They are calculated due to pressure (P) and temperature (T) as shown in Equations 3.14, 3.15 and Z can be found in Figure 3.7.

$$P_R = \frac{P}{P_c} \quad (3.14)$$

$$T_R = \frac{T}{T_c} \quad (3.15)$$

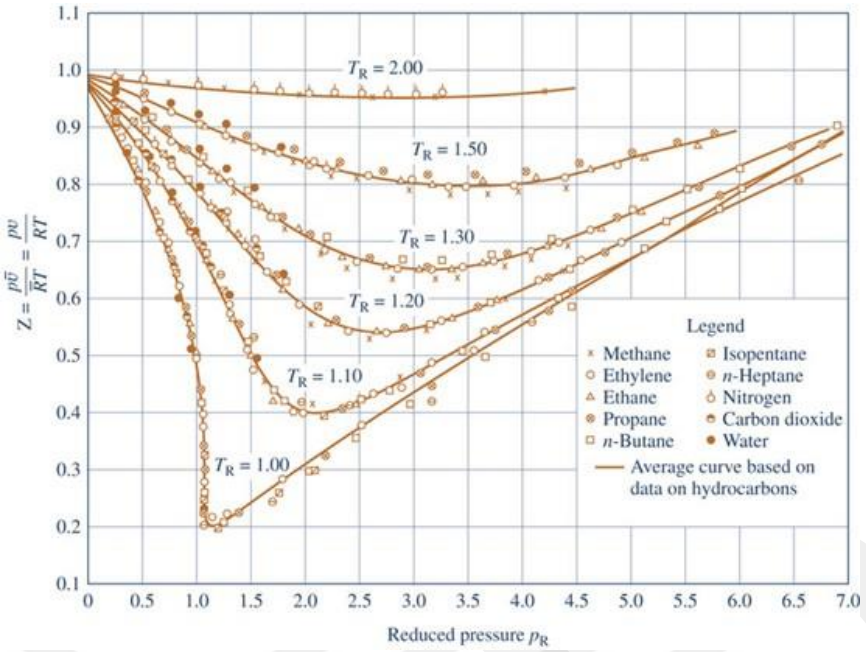

Figure 3.7: Generalized compressibility chart for various gases

Volume of gasses is calculated according to generalized compressibility chart as:

$$V = Z\frac{nRT}{P} \tag{3.16}$$

Van Der Waals derived the real gas equation from the ideal gas equation with the help of assumption of volume and pressure corrections [69]. By adding the calculated pressure drop to the real gas pressure, the ideal gas pressure and the ideal gas volume for the molecules to circulate freely by subtracting the incompressible volume calculated from the real gas volume. If it is found and written in the ideal gas equation, van der Waals equation is obtained.

$$P = \frac{nRT}{V-nb} - \frac{n^2a}{V^2} \tag{3.17}$$

Where, a is the net intermolecular attractive force and b is the finite volume of the molecules.

$$a = \frac{27}{64} \times \frac{R^2T_c^2}{P_c} \tag{3.18}$$

$$b = \frac{R}{8} \times \frac{T_c}{P_c} \tag{3.19}$$

3.4.5. CHP Calculation

The released heat during PEMFC operation is calculated in Equation 3.7. This heat should be removed with the help of cooling fluid or air cooling system. The important reasons for removing this heat is to ensure the safety of the PEMFC and increase the efficiency. Since overheating of the system can damage the materials of PEMFC and shorten its lifetime. As this heat occurs when the PEMFC generates electricity, the utilization of removed heat increases efficiency up to 90%. Transfer of this heat can be done with the help of heat exchanger (HEX) and energy balance of HEX can be calculated by Equation 3.20 [10][70]:

$$\dot{m}_{cold}.\dot{c}_{p,cold}.\left(T_{out,cold}-T_{in,cold}\right).\Delta\eta=\dot{m}_{hot}.\dot{c}_{p,hot}.\left(T_{out,hot}-T_{in,hot}\right) \quad (3.20)$$

Where $\dot{m}_{cold}$ and $\dot{m}_{hot}$ refer the mass flowrate of cooling water and heating water, respectively. $\dot{c}_{p,cold}$ and $\dot{c}_{p,hot}$ are constant specific heats of cooling and heating water. $T_{out,cold}$ and $T_{out,in}$ are cooling water outlet and inlet temperature. $T_{out,hot}$ and $T_{in,hot}$ are heating water outlet and inlet temperature. Heat exchange effectiveness of PEMFC is represented by $\Delta\eta$ and it was taken about 10% of the heat lost. Since the amount of heat to be removed is known, outlet temperatures of HEX system can be calculated as below:

$$T_{out,cold}=T_{in,cold}-\frac{q}{\dot{m}_{cold}} \quad (3.21)$$

$$T_{out,hot}=T_{in,hot}-\frac{q}{\dot{m}_{hot}} \quad (3.22)$$

3.4.6. Battery Calculation

Batteries are used to prevent undesirable power cut and to maintain H_2 production persistently. The number of batteries used in battery unit (N_{bu}) is calculated according to Dostal and Solanska. The number of batteries in one branch (N_A) is calculates as following equation:

$$N_A=\frac{V_{PV}}{V_{battery}} \quad (3.23)$$

Where V_{PV} is solar panel voltage and $V_{battery}$ is battery voltage. Due to N_A, battery

unit's branches number (N_V) is calculated by the input energy came from PV (E_{PV}), usable energy (E_{usable}) and the charging time per day (T_{HD}).

$$N_V = \frac{E_{PV}}{E_{usable} T_{HD} N_A} \tag{3.24}$$

Where E_{usable} is calculated by multiplying stored energy in battery ($E_{battery}$) and depth of discharge (H_V) as follow:

$$E_{usable} = E_{battery} H_V \tag{3.25}$$

N_{bu} is found by multiplying N_A and N_V as follow:

$$N_{bu} = N_A N_V \tag{3.26}$$

3.4.7. Economic Analysis and Levelized Cost of Energy (LCOE) Calculation

The annual real interest rate is used to convert between past cost and annual capital cost. The annual real interest rate with nominal interest rate is related to the following equation [71]:

$$i = \frac{i_0 - f}{1 + f} \tag{3.27}$$

Where i and i_o are the annual interest rate and the nominal interest rate, respectively. f denotes the annual inflation rate. Thus, in economic analysis, all costs are real costs, but the same inflation rate is accepted for all costs. Turkish Central Bank decides these values for Turkey. i_o is 10.75% in February 20, 2020 and f is 11.84% at the end of 2019. Investigating the present value of a subvention uses the capital recovery factor which is calculated due to annual real interest rate and time period (N) [72]:

$$CRF = \frac{i(1+i)^N}{(1+i)^N - 1} \tag{3.25}$$

The economic assessment is found with LCOE. Size and capacity of project, capital cost, lifetime, maintenance & operation cost change the LCOE and it is calculated as lifecycle cost of system be divided by the lifetime energy production of the system as below [73]:

$$LCOE = \frac{Lifecycle\ cost\ (\$)}{Lifetime\ energy\ production\ (kWh)} \quad (3.26)$$

Table 3.2: Economical parameters of hybrid energy system components

Component	**Capacity**	**Lifetime**	**Capital Cost ($)**	**Replacement Cost ($)**	**Operation and Maintenance Cost ($)**
PV [74]	360 W	25 yrs.	3260/kW	3260/kW	20 /year
Electrolyzer [75]	1 kW	10 yrs.	2000/kW	2000/kW	0.05/hour
PEMFC [76]	1 kW	40000 h	3000/kW	2500/kW	0.08/hour
H_2 Tank [77]	1 kg	25 yrs.	600/kg	400/kg	3/kg
Battery [78][79]	1 kW	5 yrs.	130/kW	130/kW	0.02/yrs.

CHAPTER 4

4. RESULTS

4.1.Solar Calculation Results

According to global solar irradiation and ambient temperature, P_{PV} and T_c were calculated with help of Equations 3.1 and 3.2. Simulink block diagram of P_{PV} and T_c are represented as Figure 4.1 and 4.2.

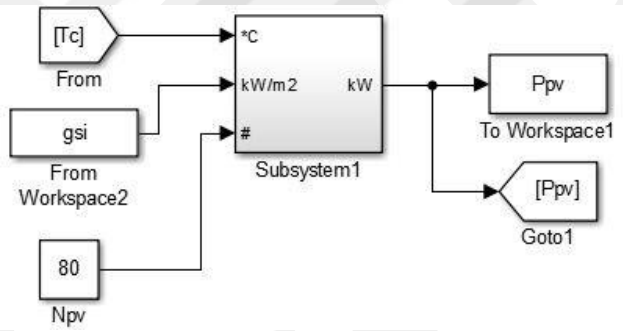

Figure 4.1: The power calculation of PV arrays in Simulink block diagram

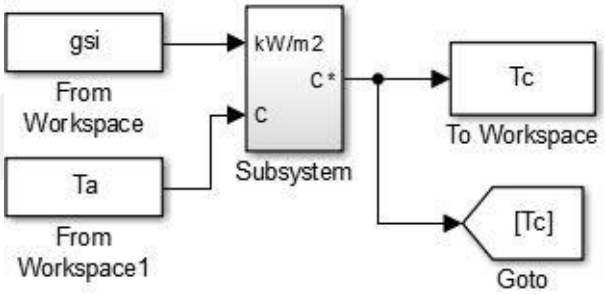

Figure 4.2: The cell temperature calculation of PV arrays in Simulink block diagram

4.2. Electrolyzer Calculation Results

When produced electricity by PV arrays is equal or more than $P_{el,min}$, electrolyzer will start operating to produce H_2. $P_{el,min}$ were calculated according to Table 3.1 with the help of Equation 3.5. $P_{el,min}$ is constant since the electrolyzer is designed. If it is desired to change its $P_{el,min}$, its voltage, current density or active area must be changed. P_{el} depends on P_{PV} and η_{dc} and were calculated in 3.7 and Simulink diagram of it as Figure 4.3.

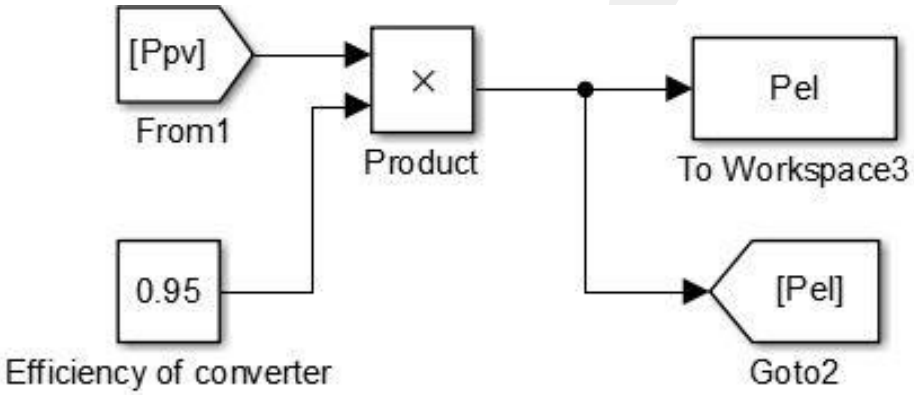

Figure 4.3: The power calculation of electrolyzer in Simulink block diagram

Since the power produced by PV changes due to ambient temperature and global solar irradiation, P_{el} will also change. The change of the P_{el} and $P_{el,min}$ for 365 days is shown in Figure 4.4. The P_{el} in some days may be less than the $P_{el,min}$.

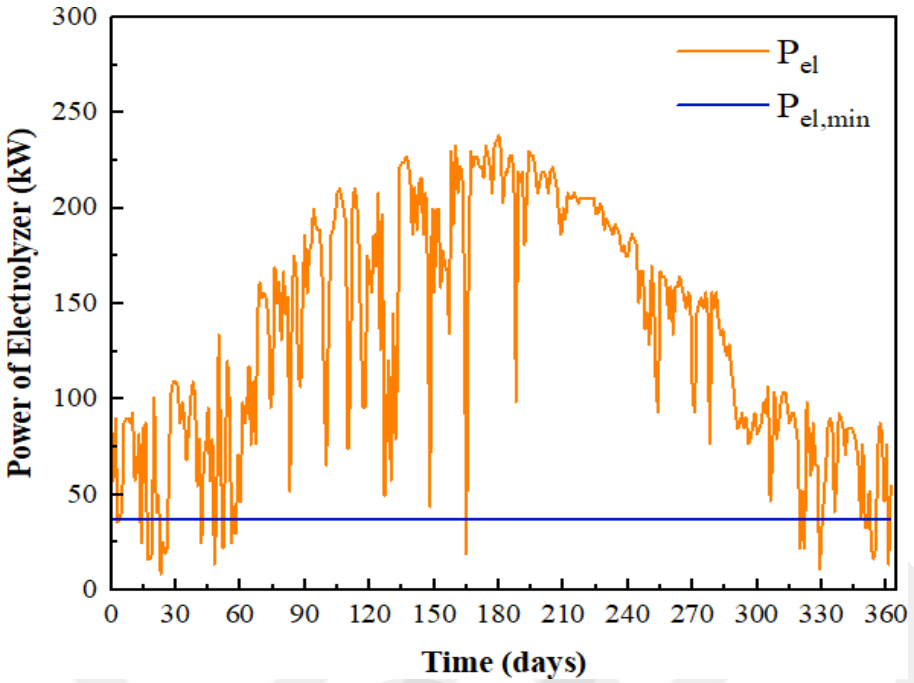

Figure 4.4: The power of electrolyzer and the minimum power of electrolyzer on daily

After calculation of P_{el}, how many kilogram H_2 was produced was found due to P_{el} by the Equation 3.6 and its Simulink diagram as shown in Figure 4.5:

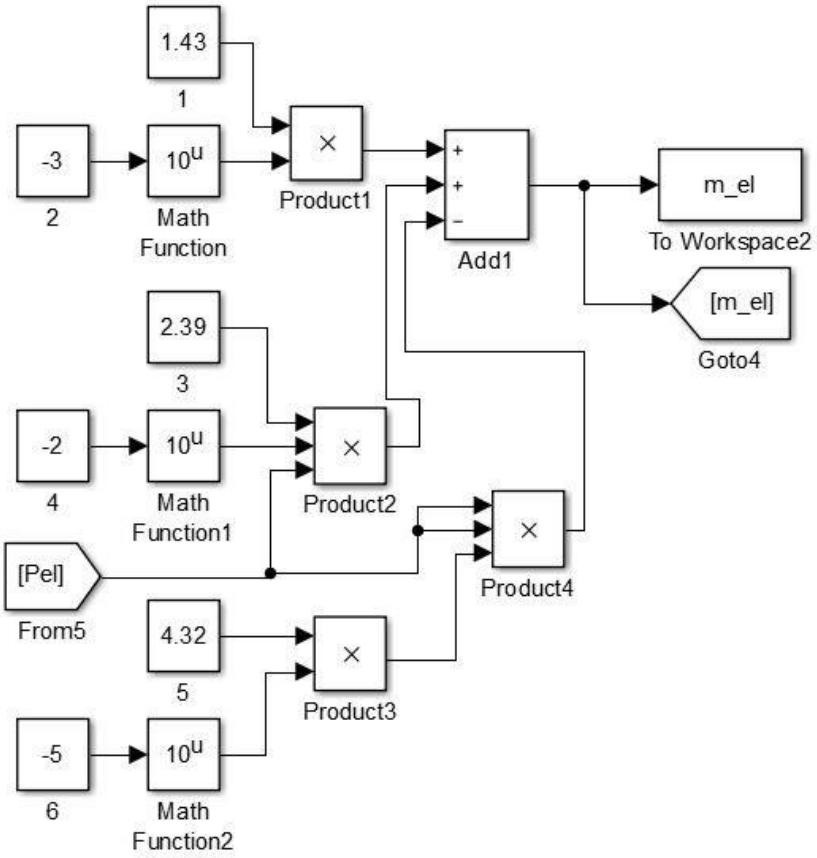

Figure 4.5: The produced H_2 calculation by electrolyzer in Simulink block diagram

The H_2 requirement of 2.4 kW PEMFC is 0.30085 g/s when it operates 5 hours in a day. The produced H_2 is subtracted from the H_2 needed by the PEMFC, excess H_2 is calculated as Figure 4.6 and stored as in Appendix A.

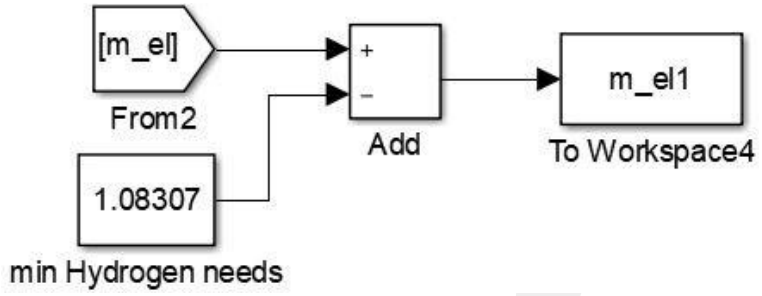

Figure 4.6: The excess H_2 calculation in Simulink block diagram

Some days the produced H_2 is less than the H_2 needed by the PEMFC. When the deficiency of H_2, it can be supplied from the H_2 tank. Thus, energy continuity is provided. Produced H_2 by electrolyzer, consumed H_2 by PEMFC and stored H_2 in tank are represented in Figure 4.7.

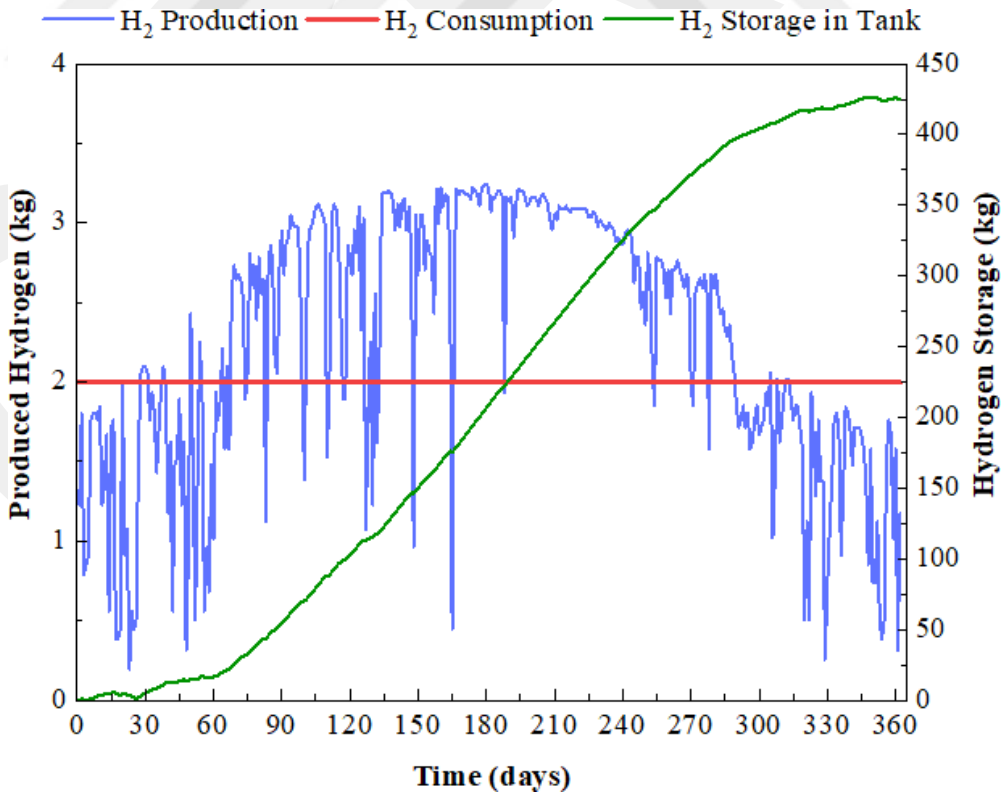

Figure 4.7: H_2 production & consumption and total H_2 storage in tank

4.3.PEMFC Results

In this thesis, 2.4 kW PEMFC was designed and parameters of it were calculated according to Table 3.1. The inlet mass flowrate amount of H_2 and the inlet mass flowrate amount of O_2, nitrogen (N_2) and water vapor in air were calculated in g/s and their Simulink diagram are shown in Figure 4.8:

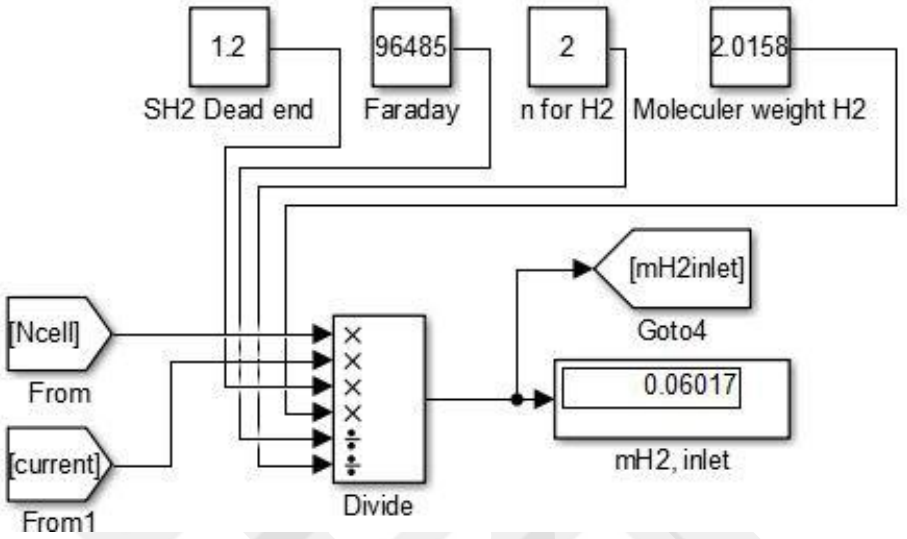

Figure 4.8: The inlet mass flowrate amount of H_2 calculation by PEMFC in Simulink block diagram

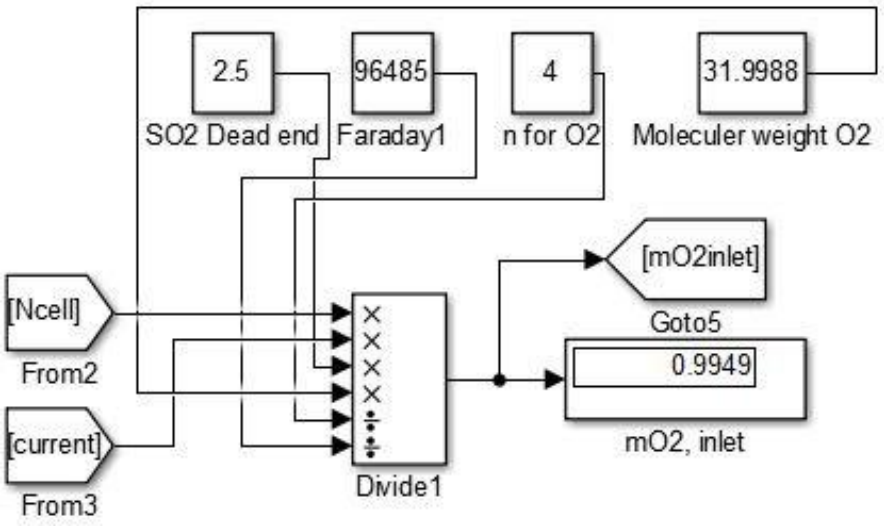

Figure 4.9: The inlet mass flowrate amount of O_2 in air calculation by PEMFC in Simulink block diagram

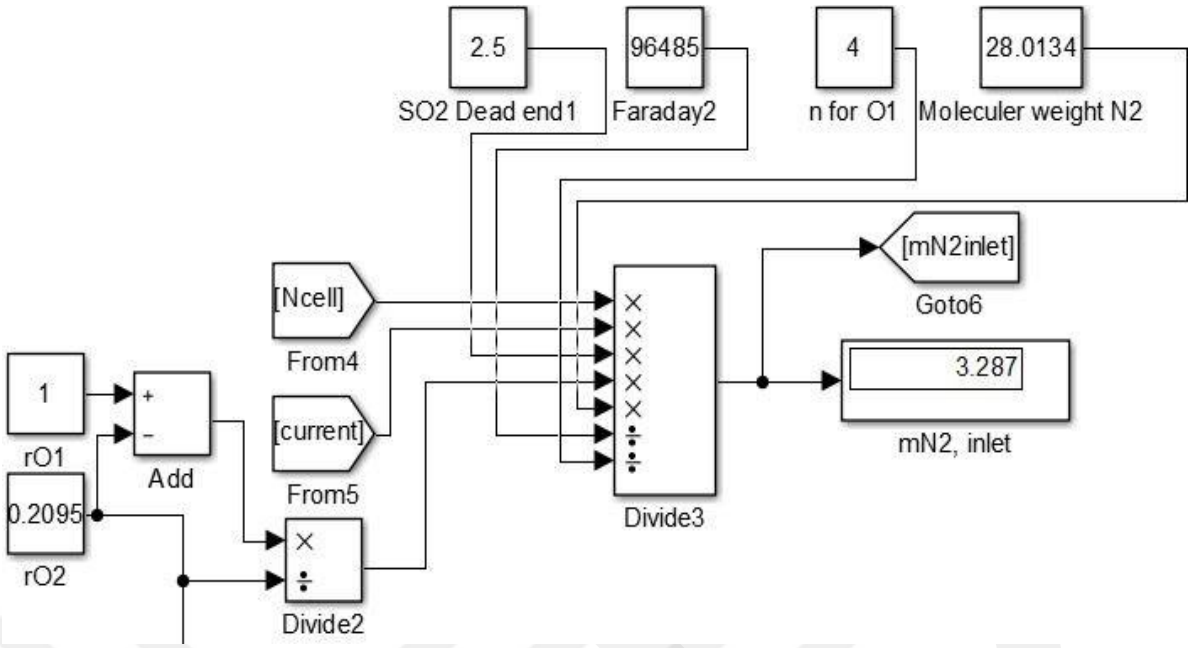

Figure 4.10: The inlet mass flowrate amount of N_2 in air calculation by PEMFC in Simulink block diagram

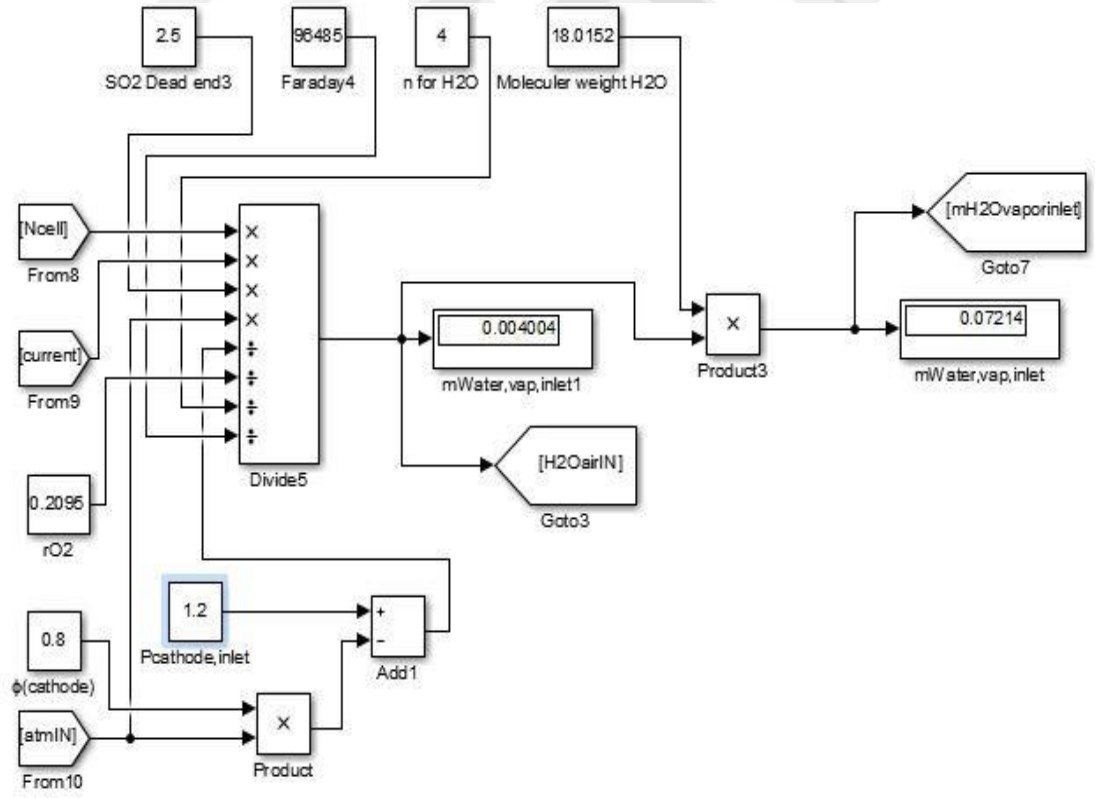

Figure 4.11: The inlet mass flowrate amount of water vapor in air calculation by PEMFC in Simulink block diagram

The outlet mass flowrate amount of H_2, O_2 and water were calculated in g/s. Since N_2 is not used in the reaction, it comes back in the amount it enters. Their Simulink diagram are shown as below:

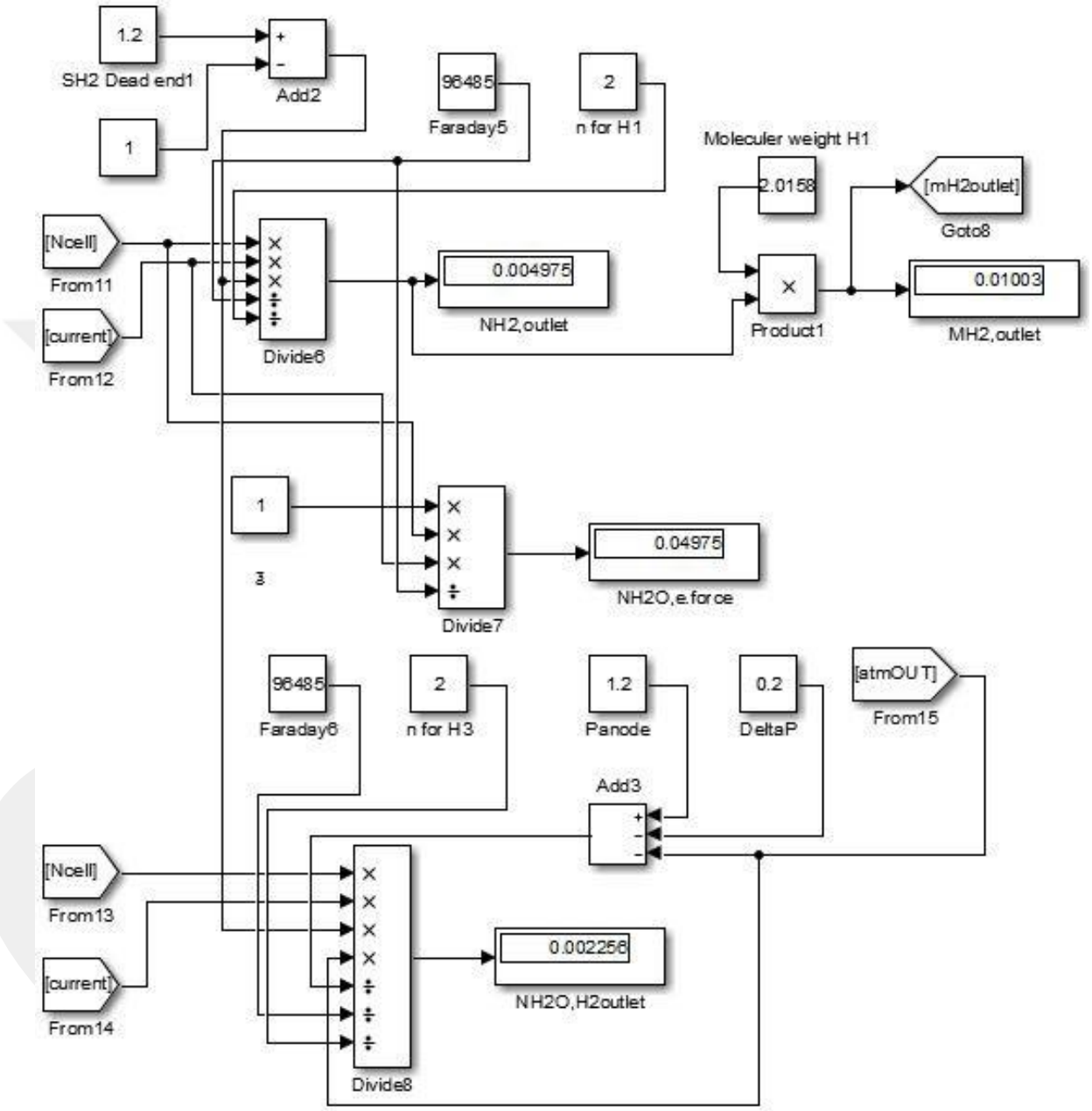

Figure 4.12: The outlet mass flowrate amount of H_2 calculation by PEMFC in Simulink block diagram

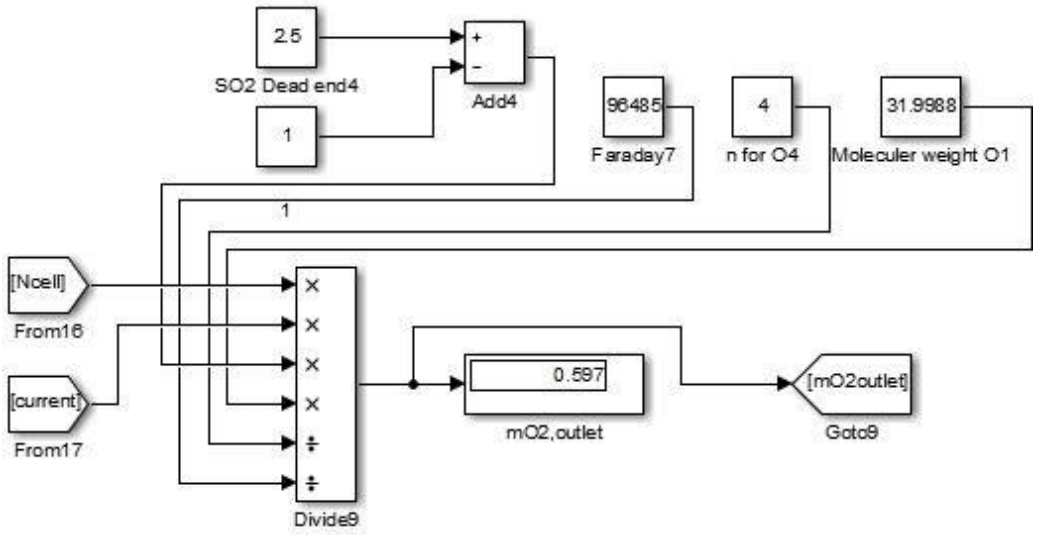

Figure 4.13: The outlet mass flowrate amount of O_2 calculation by PEMFC in Simulink block diagram

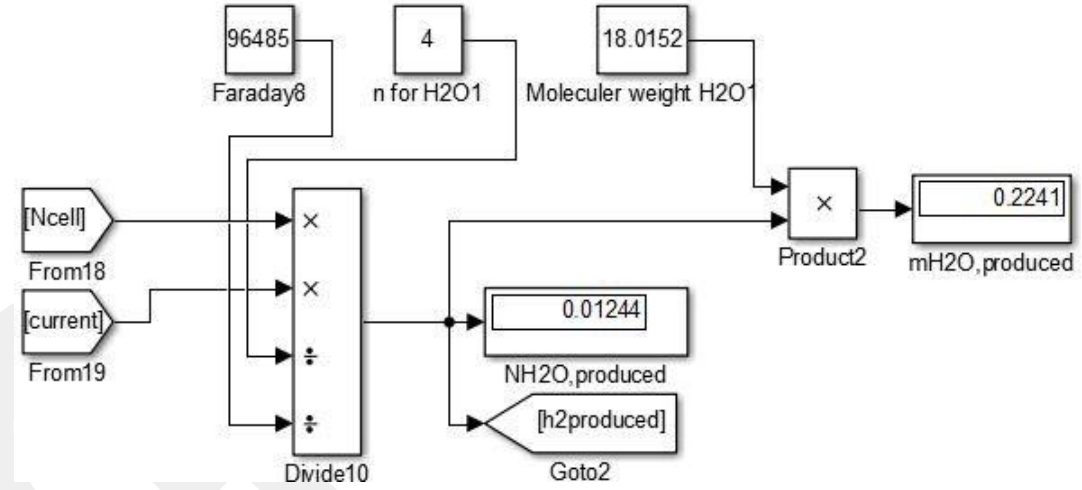

Figure 4.14: The outlet mass flowrate amount of H_2O calculation by PEMFC in Simulink block diagram

In order to find released heat from PEMFC due to Equation 3.12, total enthalpy of inlet and outlet gasses were calculated and the Simulink diagrams of these values are shown in Figure 4.15 and 4.16. The amount of released heat is shown in Figure 4.17.

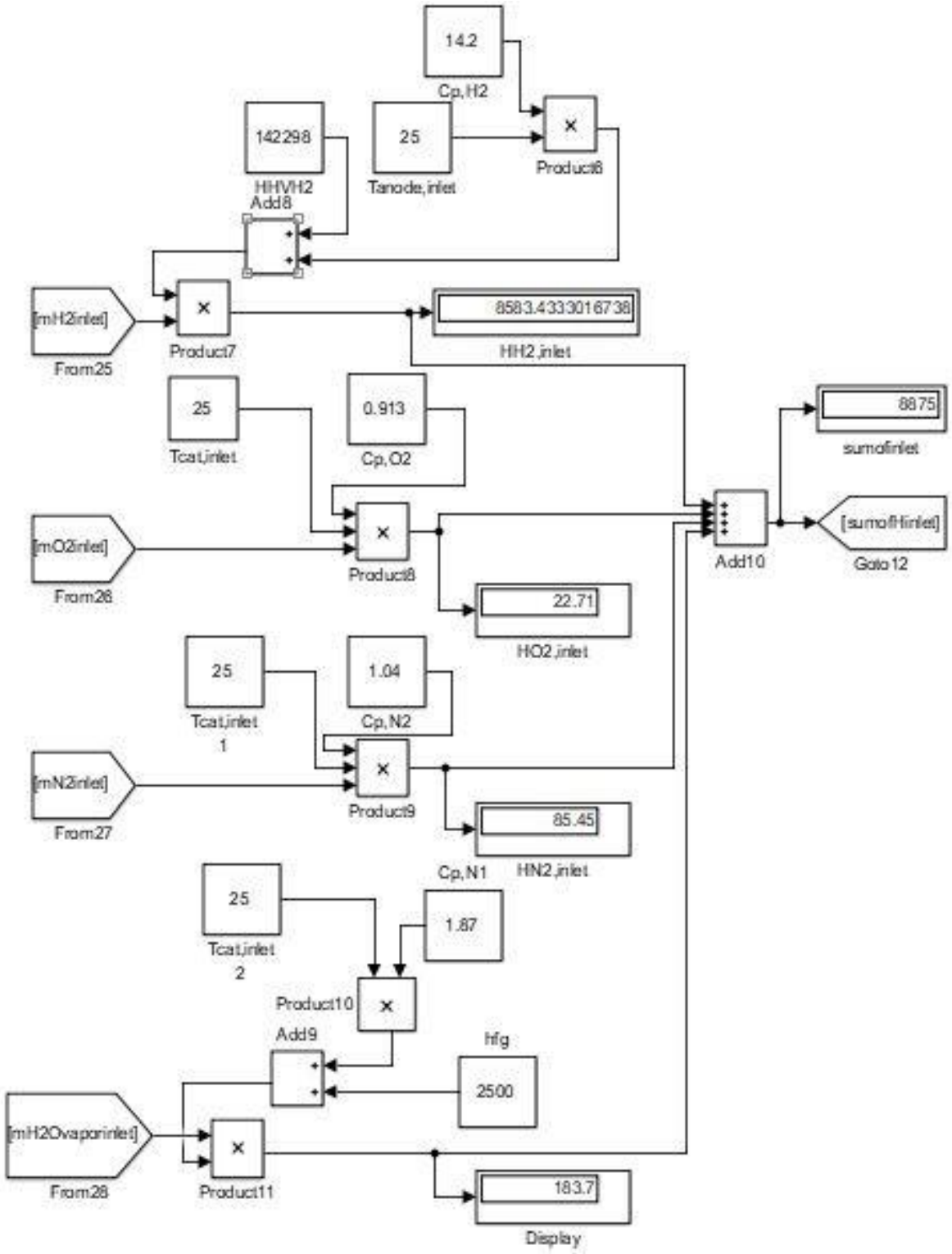

Figure 4.15: Total enthalpy of inlet gasses in Simulink block diagram

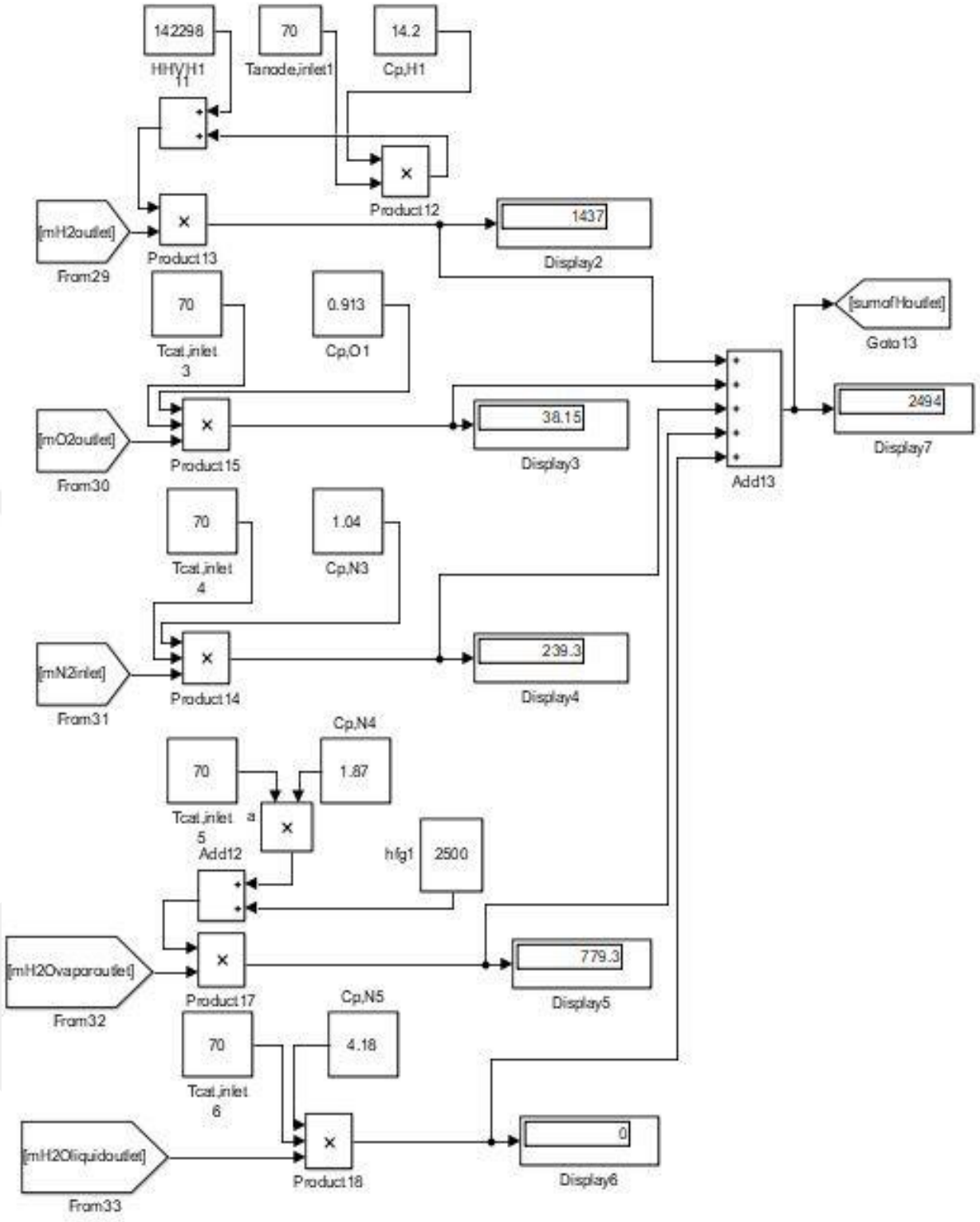

Figure 4.16: Total enthalpy of outlet gasses in Simulink block diagram

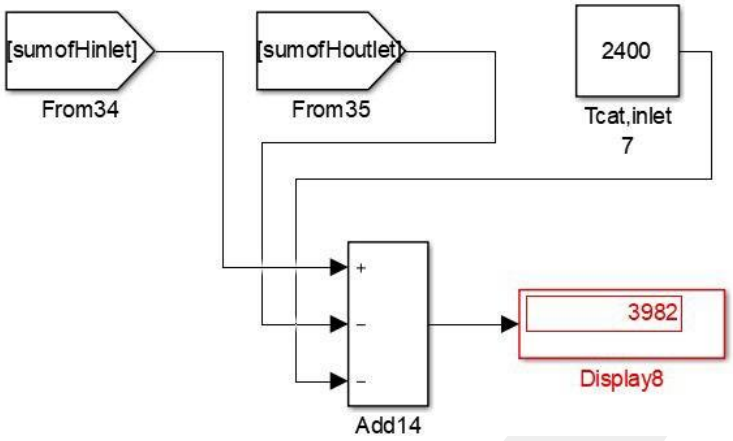

Figure 4.17: The amount of released heat calculation in Simulink block diagram

4.4.H_2 Storage Results

In this thesis, 430 kg of H_2 was compressed 35 MPa and stored 25°C. Table 4.1 shows critical pressure and temperature for some gasses [80]. a and b values in Equations 3.18,3.19 were found due to critical pressure and temperature of H_2. The result of Equation 3.17, volume of H_2 was calculated 19.33 m^3 (19330 L).

Table 4.1: Critical pressure and temperature for gasses

Gasses	**Critical Pressure (MPa)**	**Critical Temperature (K)**
Air	3.785	132.63
CO_2	7.380	304.05
CO	3.500	132.85
Ethanol	6.300	515.15
Methanol	8.100	512.60
H_2	1.300	33.20
N_2	3.040	126.15
O_2	5.050	154.55
H_2O	22.050	647.15

4.5. CHP Results

As it is seen in Figure 4.17, approximately 4 kW heat released from PEMFC when it operated an hour. In this system, PEMFC operated 5 hours in a day, so the released heat was approximately 20 kW and 10% of it was lost. Thus, 18 kW heat was rejected from the PEMFC. Assuming that $T_{in,cold}$ and $T_{in,hot}$ were 25 ^{o}C and 70^{o}C, respectively, both $\dot{m}_{cold}$ and $\dot{m}_{hot}$ were adjusted 500 g/s, $T_{out,cold}$ was found 61 ^{o}C and $T_{out,hot}$ was found 34 ^{o}C due to Equations 3.21 and 3.22.

The greenhouse was heated with coal. 500 tons of coal was taken annually for heating. Its caloric value was 6800 kJ and only 70% of it was burning when the heater was working, temperature of heater was kept constant at 60 ^{o}C.

In addition to generating electricity with proposed hybrid energy system, it had prevented the use of coal with its heat output. Thus, a self-sufficient system had been designed.

4.6. Battery Results

In this proposed hybrid system, battery calculations can be made for many possible power transmission methods. One of the method that requires the most power to be stored in the battery is that, all of the energy produced from the PV when electrolyzer does not work. Another method is to store the energy produced by PEMFC. The absence of the sun, energy is produced with stored H_2.

According to Equation 3.1, the maximum power produced by PV was approximately 250 kW on July,2. The sunshine duration of this month was 12.42 hour [81]. Assuming that the battery will be charged as much as the sunshine duration, T_{HD} can be taken as 12.42. Using Equations 3.23-3.26 and due to battery characteristic, one battery was calculated to be sufficient. When the same process was done for the power of the PEMFC, one battery was calculated to be sufficient too. In other words, in the proposed system, two batteries were designed to meet electricity need of the greenhouse in case of a possible power outage**.**

4.7. LCOE Results

The rated power, lifetime, capital, replacement and operation& maintenance costs of hybrid energy system components are represented in Table 3.2. According to the nominal interest rate and the annual inflation rate of Turkey, the annual real interest rate was found 0.97%. The lifetime of the hybrid energy system was chosen 20 years (N). Thus,CRF was calculated as 0.97 by Equation 3.24.

- Total capital cost of system is 419638 $.
- Total operation& maintenance cost of system is 6435.4 $ for 20 years.
- The total energy production is 233338.2368 kWh for 20 years. 73000 kWh energy comes from PEMFC, 146000 kW energy comes from heating, 14338.2368 kWh energy comes from H_2 tank.

Due to economic analysis, LCOE value of the hybrid energy system is 1.77 $/kWh.

Table 4.2: The economic analysis of coal system [82]

Contents	**Value**
Capacity factor (%)	85
Plant lifetime (year)	20
Fixed Operating and maintenance cost (%)	3
Variable operating and maintenance cost (%)	0.3
Coal price ($/ton)	185

The present system LCOE analysis was made according to Table 4.1 for 20 years.

- System electrical bill is approximately 6000 $.
- 350 ton of coal is 64750000 $.

Due to capacity factor, fixed and variable operating and maintenance costs of coal system is 2479544.118 $.

Total energy production came from coal boiler is 37034884 kWh for 20 years.

Due to economic analysis, LCOE value of the coal energy system is 2.06 $/kWh.

If we compare the present system with proposed hybrid system due to their LCOE, it is investigated that proposed hybrid system is more economic than coal energy system.

CHAPTER 5

5. CONCLUSION

Renewable energy sources; they emerge as environmentally friendly, modular, non-external sources in terms of reserves such as conventional sources. Due to these properties, studies on its resources gain importance day by day in our country and all over the world.

The energy obtained from renewable energy sources is due to the high investment cost, it is necessary to reach maximum efficiency during production and consumption. One way to maximize efficiency is to use more than one renewable energy sources together. Consumption of energy where it is produced is extremely important in terms of energy efficiency. In recent years, PV based Hydrogen production for PEMFCs application is a good alternative to overcome difficulties in energy storage.

In the scope of the thesis, the PV-electrolyzer-PEMFC-cogeneration hybrid energy system was designed to meet energy demand of the greenhouse. The hybrid system design was performed with MATLAB/Simulink. Firstly, electricity and heat demand of the greenhouse were determined. According to them, the PEMFC was designed as 2.4 kW to meet the need for electricity, as well as to provide the heating requirement of the greenhouse. After that, the electrolyzer was designed to supply the H_2 requirement of the PEMFC. For this purpose, the electricity demand of the electrolyzer was met from 80 PV cells. The produced H_2 was stored in storage tanks to be utilized by the PEMFC when the PV energy fail to supply the load demand. The amount of generated electricity by PV cells were calculated global solar irradiation and ambient temperature data of Şanlıurfa for 365 days. Due to the variability of the data from day to day, generated electricity changed. So the amount of H_2 produced by the electrolyzer also changed. According to the results, approximately 430 kg of H_2 was obtained and stored at the end of 365 days. Approximately 20 kW of heat had to be removed from the 2.4 kW fuel cell operated 5 hours a day. While coal was burned coal for

heating of greenhouse, the use rejected heat would raise the need for coal. In other words, integrated CHP system reduced the dependence on fossil fuel, as well as meet electricity and heat demand and increase the energy efficiency of the system.

The results demonstrate that the potential of the PV-PEMFC hybrid system for use in micro-cogeneration applications. In the future, efficiency of CHP application can be increased by using high temperature PEMFC based hybrid systems.

REFERENCES

[1] S. Pfenninger, J. DeCarolis, L. Hirth, S. Quoilin, and I. Staffell, "The importance of open data and software: Is energy research lagging behind?," *Energy Policy*, 2017, doi: 10.1016/j.enpol.2016.11.046.

[2] J. Twidell, *Renewable Energy Resources*. 2015.

[3] A. G. Olabi, "Renewable energy and energy storage systems," *Energy*. 2017, doi: 10.1016/j.energy.2017.07.054.

[4] A. Kaabeche, S. Diaf, and R. Ibtiouen, "Firefly-inspired algorithm for optimal sizing of renewable hybrid system considering reliability criteria," *Sol. Energy*, 2017, doi: 10.1016/j.solener.2017.06.070.

[5] P. Arun, R. Banerjee, and S. Bandyopadhyay, "Optimum sizing of photovoltaic battery systems incorporating uncertainty through design space approach," *Sol. Energy*, 2009, doi: 10.1016/j.solener.2009.01.003.

[6] Y. Zhang, A. Lundblad, P. E. Campana, F. Benavente, and J. Yan, "Battery sizing and rule-based operation of grid-connected photovoltaic-battery system: A case study in Sweden," *Energy Convers. Manag.*, 2017, doi: 10.1016/j.enconman.2016.11.060.

[7] J. Lagorse, D. Paire, and A. Miraoui, "Sizing optimization of a stand-alone street lighting system powered by a hybrid system using fuel cell, PV and battery," *Renew. Energy*, 2009, doi: 10.1016/j.renene.2008.05.030.

[8] J. J. Hwang, L. K. Lai, W. Wu, and W. R. Chang, "Dynamic modeling of a photovoltaic hydrogen fuel cell hybrid system," *Int. J. Hydrogen Energy*, 2009, doi: 10.1016/j.ijhydene.2009.09.100.

[9] T. M. I. Mahlia and P. L. Chan, "Life cycle cost analysis of fuel cell based cogeneration system for residential application in Malaysia," *Renewable and Sustainable Energy Reviews*. 2011, doi: 10.1016/j.rser.2010.07.041.

[10] A. Hajatzadeh Pordanjani, S. Aghakhani, M. Afrand, B. Mahmoudi, O. Mahian, and S. Wongwises, "An updated review on application of nanofluids in heat exchangers for saving energy," *Energy Conversion and Management*. 2019, doi: 10.1016/j.enconman.2019.111886.

[11] V. V. Tyagi, N. A. A. Rahim, N. A. Rahim, and J. A. /L. Selvaraj, "Progress in

solar PV technology: Research and achievement," *Renew. Sustain. Energy Rev.*, vol. 20, pp. 443–461, Apr. 2013, doi: 10.1016/J.RSER.2012.09.028.

[12] M. Rashad, A. A. El-Samahy, M. Daowd, and A. M. A. Amin, "A comparative Study on Photovoltaic and Concentrated Solar Thermal Power Plants," *Recent Adv. Environ. Earth Sci. Econ.*, 2013.

[13] R. Daneshpour and M. Mehrpooya, "Design and optimization of a combined solar thermophotovoltaic power generation and solid oxide electrolyser for hydrogen production," *Energy Convers. Manag.*, vol. 176, pp. 274–286, Nov. 2018, doi: 10.1016/J.ENCONMAN.2018.09.033.

[14] T. Salmi, M. Bouzguenda, A. Gastli, and A. Masmoudi, "MATLAB/simulink based modelling of solar photovoltaic cell," *Int. J. Renew. Energy Res.*, 2012, doi: 10.20508/ijrer.42248.

[15] C. Author *et al.*, "Natural and environment favourable Dye Used as Light Sensitizer in Dye Sensitized Solar Cell: A Critical Review," *J. Mater. Sci. Surf. Eng.*, 2017.

[16] P. Rajput, G. N. Tiwari, O. S. Sastry, B. Bora, and V. Sharma, "Degradation of mono-crystalline photovoltaic modules after 22 years of outdoor exposure in the composite climate of India," *Sol. Energy*, 2016, doi: 10.1016/j.solener.2016.06.047.

[17] W. Xiao, W. G. Dunford, and A. Capel, "A novel modeling method for photovoltaic cells," in *PESC Record - IEEE Annual Power Electronics Specialists Conference*, 2004, doi: 10.1109/PESC.2004.1355416.

[18] C. Konstantopoulos and E. Koutroulis, "Global maximum power point tracking of flexible photovoltaic modules," *IEEE Trans. Power Electron.*, 2014, doi: 10.1109/TPEL.2013.2275947.

[19] W. Shockley, "The Theory of p-n Junctions in Semiconductors and p-n Junction Transistors," *Bell Syst. Tech. J.*, 1949, doi: 10.1002/j.1538-7305.1949.tb03645.x.

[20] A. Shukla, M. Khare, and K. N. Shukla, "Modeling and Simulation of Solar PV Module on MATLAB/Simulink," *Int. J. Innov. Res. Sci. Eng. Technol.*, 2015, doi: 10.15680/ijirset.2015.0401015.

[21] M. H. El-Ahmar, A. H. M. El-Sayed, and A. M. Hemeida, "Mathematical modeling of Photovoltaic module and evalute the effect of varoius paramenters on its performance," in *2016 18th International Middle-East Power Systems Conference,*

MEPCON 2016 - Proceedings, 2017, doi: 10.1109/MEPCON.2016.7836976.

[22] J. Rossmeisl, Z. W. Qu, H. Zhu, G. J. Kroes, and J. K. Nørskov, "Electrolysis of water on oxide surfaces," *J. Electroanal. Chem.*, 2007, doi: 10.1016/j.jelechem.2006.11.008.

[23] I. Dincer and C. Acar, "Review and evaluation of hydrogen production methods for better sustainability," *Int. J. Hydrogen Energy*, 2014, doi: 10.1016/j.ijhydene.2014.12.035.

[24] H. A. Khater, A. A. Abdelraouf, and M. H. Beshr, "Optimum Alkaline Electrolyzer-Proton Exchange Membrane Fuel Cell Coupling in a Residential Solar Stand-Alone Power System," *ISRN Renew. Energy*, 2011, doi: 10.5402/2011/953434.

[25] J. Larminie, *Fuel cell system explained*, Second., vol. 34, no. 11. 2003.

[26] A. Züttel, "Materials for hydrogen storage," *Mater. Today*, 2003, doi: 10.1016/S1369-7021(03)00922-2.

[27] J. Larminie and A. Dicks, *Fuel cell systems explained: Second edition*. 2013.

[28] F. Barbir, *Pem Fuel Cells: Theory and Practice (2nd Edition)*. 2012.

[29] M. Warshay and P. R. Prokopius, "The fuel cell in space: yesterday, today and tomorrow," *J. Power Sources*, 1990, doi: 10.1016/0378-7753(90)80019-A.

[30] S. Mekhilef, R. Saidur, and A. Safari, "Comparative study of different fuel cell technologies," *Renewable and Sustainable Energy Reviews*. 2012, doi: 10.1016/j.rser.2011.09.020.

[31] C. Spiegel, *Designing and Building Fuel Cells*. 2007.

[32] H. A. Hamedani *et al.*, "Microstructure, property and processing relation in gradient porous cathode of solid oxide fuel cells using statistical continuum mechanics," *J. Power Sources*, 2011, doi: 10.1016/j.jpowsour.2011.03.046.

[33] A. O. Isenberg, "Energy conversion via solid oxide electrolyte electrochemical cells at high temperatures," *Solid State Ionics*, 1981, doi: 10.1016/0167-2738(81)90127-2.

[34] A. L. Dicks, "Molten carbonate fuel cells," *Curr. Opin. Solid State Mater. Sci.*, 2004, doi: 10.1016/j.cossms.2004.12.005.

[35] G. Hoogers, *Fuel cell technology handbook*. 2002.

[36] S. Lu, J. Pan, A. Huang, L. Zhuang, and J. Lu, "Alkaline polymer electrolyte fuel cells completely free from noble metal catalysts," *Proc. Natl. Acad. Sci. U. S. A.*, 2008, doi: 10.1073/pnas.0810041106.

[37] N. Sammes, R. Bove, and K. Stahl, “Phosphoric acid fuel cells: Fundamentals and applications,” *Curr. Opin. Solid State Mater. Sci.*, 2004, doi: 10.1016/j.cossms.2005.01.001.

[38] S. Yerramalla, A. Davari, A. Feliachi, and T. Biswas, “Modeling and simulation of the dynamic behavior of a polymer electrolyte membrane fuel cell,” *J. Power Sources*, 2003, doi: 10.1016/S0378-7753(03)00733-X.

[39] J. M. Andújar and F. Segura, “Fuel cells: History and updating. A walk along two centuries,” *Renewable and Sustainable Energy Reviews*. 2009, doi: 10.1016/j.rser.2009.03.015.

[40] L. Wang, A. Husar, T. Zhou, and H. Liu, “A parametric study of PEM fuel cell performances,” *Int. J. Hydrogen Energy*, 2003, doi: 10.1016/S0360-3199(02)00284-7.

[41] M. Borah and S. Dhakate, “Expanded Graphite Composite Based Bipolar Plate for PEM Fuel Cell: Development of Low Density and Low Cost Composite Bipolar Plate for Proton Exchange Membrane Fuel Cell,” *Lambert Acad. Publ.*, 2016.

[42] G. Y. Choe, J. S. Kim, H. S. Kang, B. K. Lee, and W. Y. Lee, “Proton exchange membrane fuel cell (PEMFC) modeling for high efficiency fuel cell balance of plant (BOP),” in *Proceeding of International Conference on Electrical Machines and Systems, ICEMS 2007*, 2007, doi: 10.1109/ICEMS.2007.4412239.

[43] M. Derbeli, O. Barambones, and L. Sbita, “A robust maximum power point tracking control method for a PEM fuel cell power system,” *Appl. Sci.*, 2018, doi: 10.3390/app8122449.

[44] M. Derbeli, M. Farhat, O. Barambones, and L. Sbita, “Control of PEM fuel cell power system using sliding mode and super-twisting algorithms,” *Int. J. Hydrogen Energy*, 2017, doi: 10.1016/j.ijhydene.2016.06.103.

[45] J. H. Jung and S. Ahmed, “Dynamic model of PEM fuel cell using real-time simulation techniques,” *J. Power Electron.*, 2010, doi: 10.6113/JPE.2010.10.6.739.

[46] H. Liu, Y. Shao, and J. Li, “A biomass-fired micro-scale CHP system with organic Rankine cycle (ORC) - Thermodynamic modelling studies,” *Biomass and Bioenergy*, 2011, doi: 10.1016/j.biombioe.2011.06.025.

[47] M. Dentice d’Accadia, M. Sasso, S. Sibilio, and L. Vanoli, “Micro-combined heat and power in residential and light commercial applications,” *Appl. Therm. Eng.*, 2003, doi: 10.1016/S1359-4311(03)00030-9.

[48] H. Nasiraghdam and S. Jadid, “Optimal hybrid PV/WT/FC sizing and distribution system reconfiguration using multi-objective artificial bee colony (MOABC) algorithm,” *Sol. Energy*, 2012, doi: 10.1016/j.solener.2012.07.014.

[49] M. Eroglu, E. Dursun, S. Sevencan, J. Song, S. Yazici, and O. Kilic, “A mobile renewable house using PV/wind/fuel cell hybrid power system,” *Int. J. Hydrogen Energy*, 2011, doi: 10.1016/j.ijhydene.2011.01.046.

[50] C. Ghenai, T. Salameh, and A. Merabet, “Technico-economic analysis of off grid solar PV/Fuel cell energy system for residential community in desert region,” *Int. J. Hydrogen Energy*, 2020, doi: 10.1016/j.ijhydene.2018.05.110.

[51] T. Lajnef, S. Abid, and A. Ammous, “Modeling, control, and simulation of a solar hydrogen/fuel cell hybrid energy system for grid-connected applications,” *Advances in Power Electronics*. 2013, doi: 10.1155/2013/352765.

[52] E. Özgirgin, Y. Devrim, and A. Albostan, “Modeling and simulation of a hybrid photovoltaic (PV) module-electrolyzer-PEM fuel cell system for micro-cogeneration applications,” in *International Journal of Hydrogen Energy*, 2015, doi: 10.1016/j.ijhydene.2015.06.122.

[53] N. M. Isa, H. S. Das, C. W. Tan, A. H. M. Yatim, and K. Y. Lau, “A techno-economic assessment of a combined heat and power photovoltaic/fuel cell/battery energy system in Malaysia hospital,” *Energy*, 2016, doi: 10.1016/j.energy.2016.06.056.

[54] A. Ganguly, D. Misra, and S. Ghosh, “Modeling and analysis of solar photovoltaic-electrolyzer-fuel cell hybrid power system integrated with a floriculture greenhouse,” *Energy Build.*, vol. 42, no. 11, pp. 2036–2043, Nov. 2010, doi: 10.1016/J.ENBUILD.2010.06.012.

[55] A. Satchwell, P. Cappers, and C. Goldman, “Customer bill impacts of energy efficiency and net-metered photovoltaic system investments,” *Util. Policy*, vol. 50, pp. 144–152, Feb. 2018, doi: 10.1016/J.JUP.2017.12.003.

[56] C. Yan, S. Wang, and F. Xiao, “A simplified energy performance assessment method for existing buildings based on energy bill disaggregation,” *Energy Build.*, 2012, doi: 10.1016/j.enbuild.2012.09.043.

[57] E. Alizadeh, S. M. Rahgoshay, M. Rahimi-Esbo, M. Khorshidian, and S. H. M. Saadat, “A novel cooling flow field design for polymer electrolyte membrane fuel cell stack,” *Int. J. Hydrogen Energy*, vol. 41, no. 20, pp. 8525–8532, Jun. 2016, doi:

10.1016/J.IJHYDENE.2016.03.187.

[58] G. Zhang and S. G. Kandlikar, “A critical review of cooling techniques in proton exchange membrane fuel cell stacks,” *Int. J. Hydrogen Energy*, vol. 37, no. 3, pp. 2412–2429, Feb. 2012, doi: 10.1016/J.IJHYDENE.2011.11.010.

[59] V. Mertens *et al.*, “21.4 % EFFICIENT FULLY SCREEN PRINTED N-TYPE SOLAR CELL ON EPITAXIALLY GROWN SILICON WAFERS WITH BUILT-IN BORON REAR SIDE EMITTER,” in *31st European Photovoltaics Solar Energy Conference and Exhibition*, 2015.

[60] Y. Devrim and L. Bilir, “Performance investigation of a wind turbine–solar photovoltaic panels–fuel cell hybrid system installed at İncek region – Ankara, Turkey,” *Energy Convers. Manag.*, 2016, doi: 10.1016/j.enconman.2016.08.062.

[61] Y. Budak and Y. Devrim, “Investigation of micro-combined heat and power application of PEM fuel cell systems,” *Energy Convers. Manag.*, vol. 160, pp. 486–494, Mar. 2018, doi: 10.1016/j.enconman.2018.01.077.

[62] N. Agarwal, A. Kumar, and Varun, “Optimization of grid independent hybrid PV-diesel-battery system for power generation in remote villages of Uttar Pradesh, India,” *Energy Sustain. Dev.*, 2013, doi: 10.1016/j.esd.2013.02.002.

[63] “Turkey - Lessons - Tes Teach.” https://www.tes.com/lessons/ziLIrzl5Sg2F0Q/turkey (accessed Jun. 08, 2020).

[64] M. Kacira, M. Simsek, Y. Babur, and S. Demirkol, “Determining optimum tilt angles and orientations of photovoltaic panels in Sanliurfa, Turkey,” *Renew. Energy*, vol. 29, no. 8, pp. 1265–1275, Jul. 2004, doi: 10.1016/J.RENENE.2003.12.014.

[65] H. Tebibel, S. Menia, and A. Khellaf, “Off grid PV system for hydrogen production using methanol electrolysis and an optimal management strategy,” *Proc. 2016 Int. Renew. Sustain. Energy Conf. IRSEC 2016*, pp. 999–1004, 2017, doi: 10.1109/IRSEC.2016.7983941.

[66] B. Han, S. M. Steen, J. Mo, and F. Y. Zhang, “Electrochemical performance modeling of a proton exchange membrane electrolyzer cell for hydrogen energy,” *Int. J. Hydrogen Energy*, 2015, doi: 10.1016/j.ijhydene.2015.03.164.

[67] Z. Bak Kibar, F. Yaman, and A. Ayas, “Assessing prospective chemistry teachers’ understanding of gases through qualitative and quantitative analyses of their concept maps,” *Chem. Educ. Res. Pract.*, 2013, doi: 10.1039/c3rp00052d.

[68] M. A. Mahmoud, “Development of a new correlation of gas compressibility

factor (Z-factor) for high pressure gas reservoirs," in *Society of Petroleum Engineers - North Africa Technical Conference and Exhibition 2013, NATC 2013*, 2013, doi: 10.1115/1.4025019.

[69] E. E. Shpilrain, "VAN DER WAALS EQUATION OF STATE," *A-to-Z Guid. to Thermodyn. Heat Mass Transf. Fluids Eng.*, 2006, doi: 10.1615/atoz.v.vanderwaaequofsta.

[70] Y. A. Cengel and M. A. Boles, *Thermodynamics: an Engineering Approach 8th Edition*. 2015.

[71] S. Rahimi, M. Meratizaman, S. Monadizadeh, and M. Amidpour, "Techno-economic analysis of wind turbine–PEM (polymer electrolyte membrane) fuel cell hybrid system in standalone area," *Energy*, vol. 67, pp. 381–396, Apr. 2014, doi: 10.1016/J.ENERGY.2014.01.072.

[72] M. A. V. Rad, R. Ghasempour, P. Rahdan, S. Mousavi, and M. Arastounia, "Techno-economic analysis of a hybrid power system based on the cost-effective hydrogen production method for rural electrification, a case study in Iran," *Energy*, vol. 190, p. 116421, Jan. 2020, doi: 10.1016/J.ENERGY.2019.116421.

[73] C. S. Lai and M. D. McCulloch, "Levelized cost of electricity for solar photovoltaic and electrical energy storage," *Appl. Energy*, vol. 190, pp. 191–203, Mar. 2017, doi: 10.1016/J.APENERGY.2016.12.153.

[74] S. Mandal, B. K. Das, and N. Hoque, "Optimum sizing of a stand-alone hybrid energy system for rural electrification in Bangladesh," *J. Clean. Prod.*, vol. 200, pp. 12–27, Nov. 2018, doi: 10.1016/J.JCLEPRO.2018.07.257.

[75] M. Temiz and N. Javani, "Design and analysis of a combined floating photovoltaic system for electricity and hydrogen production," *Int. J. Hydrogen Energy*, vol. 45, no. 5, pp. 3457–3469, Jan. 2020, doi: 10.1016/J.IJHYDENE.2018.12.226.

[76] H. S. Das, C. W. Tan, A. H. M. Yatim, and K. Y. Lau, "Feasibility analysis of hybrid photovoltaic/battery/fuel cell energy system for an indigenous residence in East Malaysia," *Renew. Sustain. Energy Rev.*, vol. 76, pp. 1332–1347, Sep. 2017, doi: 10.1016/J.RSER.2017.01.174.

[77] M. Gökçek and C. Kale, "Techno-economical evaluation of a hydrogen refuelling station powered by Wind-PV hybrid power system: A case study for İzmir-çeşme," *Int. J. Hydrogen Energy*, 2018, doi: 10.1016/j.ijhydene.2018.01.082.

[78] D. B. Nelson, M. H. Nehrir, and C. Wang, "Unit sizing and cost analysis of

stand-alone hybrid wind/PV/fuel cell power generation systems," *Renew. Energy*, vol. 31, no. 10, pp. 1641–1656, Aug. 2006, doi: 10.1016/j.renene.2005.08.031.

[79] Y. Budak and Y. Devrim, "Comparative study of PV/PEM fuel cell hybrid energy system based on methanol and water electrolysis," *Energy Convers. Manag.*, vol. 179, pp. 46–57, 2019, doi: 10.1016/j.enconman.2018.10.053.

[80] a W. Adamson and a P. Gast, *Physical Chemistry of Surfaces Sixth Edition*. 1997.

[81] "Meteoroloji Genel Müdürlüğü." https://www.mgm.gov.tr/veridegerlendirme/il-ve-ilceler istatistik.aspx?m=SANLIURFA (accessed Jun. 16, 2020).

[82] S. H. Park, J. Y. Kim, M. K. Yoon, D. R. Rhim, and C. S. Yeom, "Thermodynamic and economic investigation of coal-fired power plant combined with various supercritical CO2 Brayton power cycle," *Appl. Therm. Eng.*, 2018, doi: 10.1016/j.applthermaleng.2017.10.145.

APPENDIX A

ALGORITHMS

A.1 Algorithm 1

The following is a MATLAB code which finds the sum of excess H_2:

```
load gsi
load Ta
hydrogen_produced=0;
for i=1:364
hydrogen_produced = m_el(i)-1.0831+hydrogen produced
end
```